VolkswagenStiftung

INRIA
November 2013

The ADER-DG method for seismology: recent technical developments and applications to earthquake rupture dynamics

Christian Pelties,

Alice Gabriel, Stefan Wenk, Martin Käser, Josep de la Puente, Alex Breuer, Alex Heinecke, Sebastian Rettenberger, Michael Bader, Atanas Atanasov, Luca Passone, Vipin Sachdeva, Martin Mai, Kirk E. Jordan, Jean-Paul Ampuero, Gilbert Brietzke, Cameron Smith, ...

LMU
LUDWIG-MAXIMILIANS-UNIVERSITÄT MÜNCHEN

Project members

LMU LUDWIG-MAXIMILIANS-UNIVERSITÄT MÜNCHEN

Coordination, Host, Physics, Numerics, Algorithm, Pre- and Postprocessing, Application, User support

TUM TECHNISCHE UNIVERSITÄT MÜNCHEN

Technical development, HPC, Optimization, Visualization, Design

IBM

Consulting, Scaling, BlueGene/Q adaption

KAUST King Abdullah University of Science and Technology

Visualization, parallel I/O

SCOREC

Automated CAD generation

Simmetrix Inc. Enabling Simulation-Based Design

Meshing, CAD generation

Caltech

ETH

BSC Barcelona Supercomputing Center Centro Nacional de Supercomputación

lrz

...and others …
Support, Guidance, Experience sharing, Consulting, ...

Goal

Complete seismic wave propagation package including solutions for

- **dynamic earthquake rupture**
- **exploration industry**
- **Seismology**

with complex geometry
and heterogeneous medium.

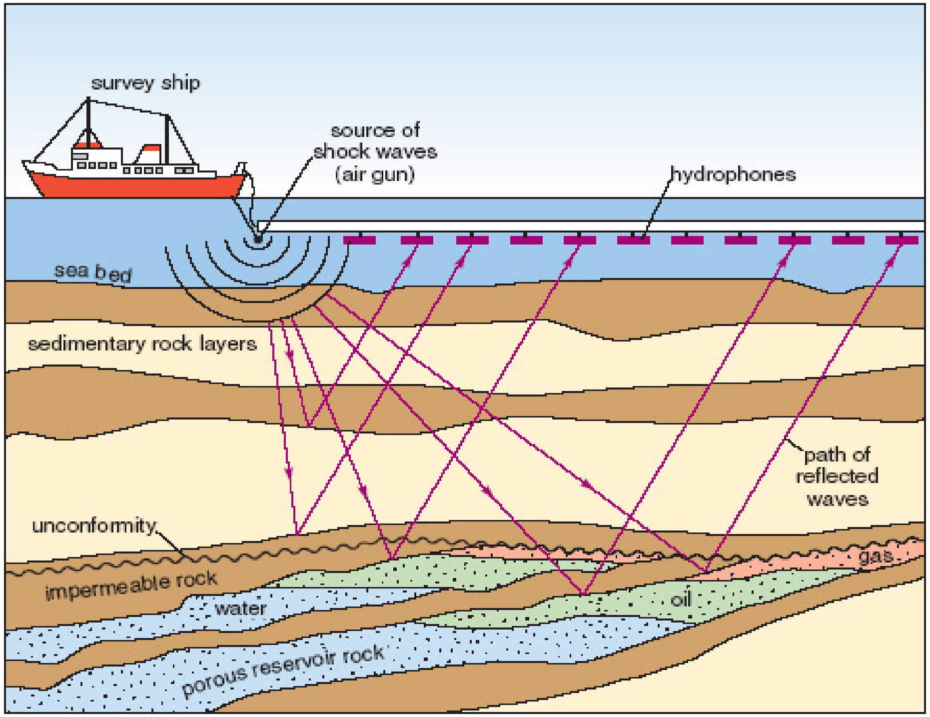

(Open University: 2002 UK Offshore Operators Association)

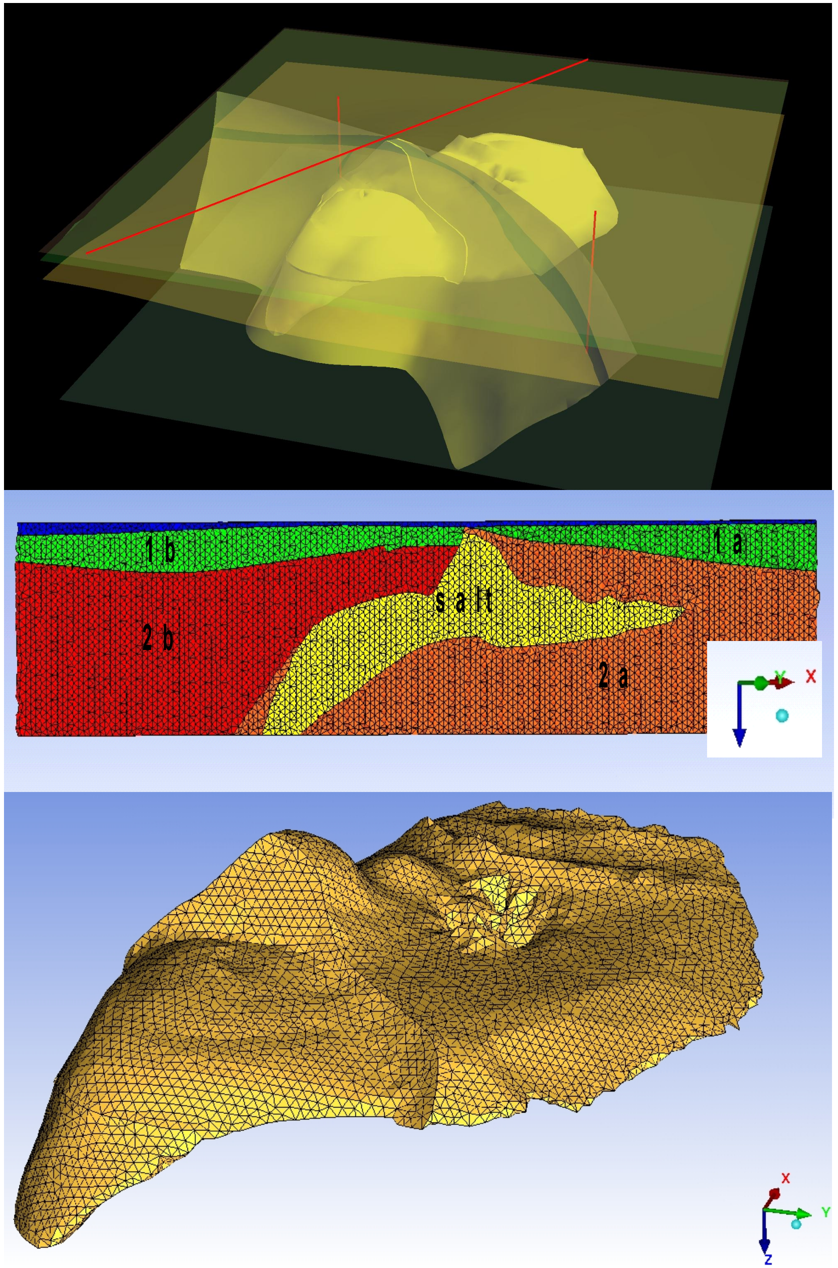

Käser, Martin, Christian Pelties, E. Cristobal Castro, Hugues Djikpesse, and Michael Prange (2010), **Wave Field Modeling in Exploration Seismology Using the Discontinuous Galerkin Finite Element Method on HPC-infrastructure**, *The Leading Edge*

Problems in understanding earthquakes

- Basic physics of earthquakes having been known since roughly a century (Gilbert [1884], Reid [1910])

- Unknowns

  e.g. how friction weakens in detail, influence of fault geometry, pressure of pore fluids within fault zones and how they respond to slip, no direct observation, ...

  → research

(Photos by courtesy of USGS)

Problems in understanding earthquakes

- Basic physics of earthquakes having been known since roughly a century (Gilbert [1884], Reid [1910])

- Unknowns

  e.g. how friction weakens in detail, influence of fault geometry, pressure of pore fluids within fault zones and how they respond to slip, no direct observation, ...

  → research

- Tools:

  - Laboratory rock experiments

  - Data (stress, microseismic activity, co- & postseismic deformation)

  - Theory

  - Numerical experiments

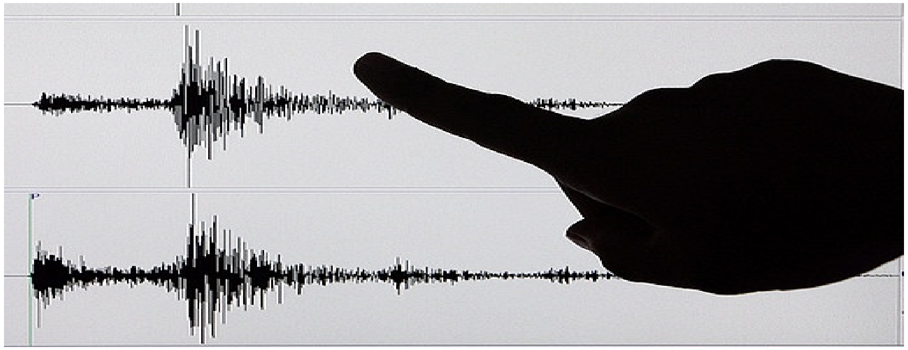

(dpa)

(Lu, Lapusta and Rosakis, 2007)

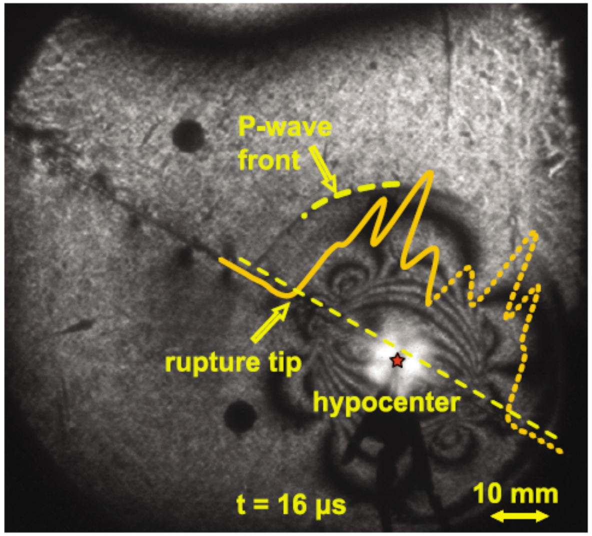

Scenario simulations

- Large-scale numerical earthquake scenario simulations can improve physics-based predictions
    - Complex (realistic) dynamic ruptures in 3D Earth structure
    - Ground-motion generation and propagation
    - Data-intensive petascale computing and storage

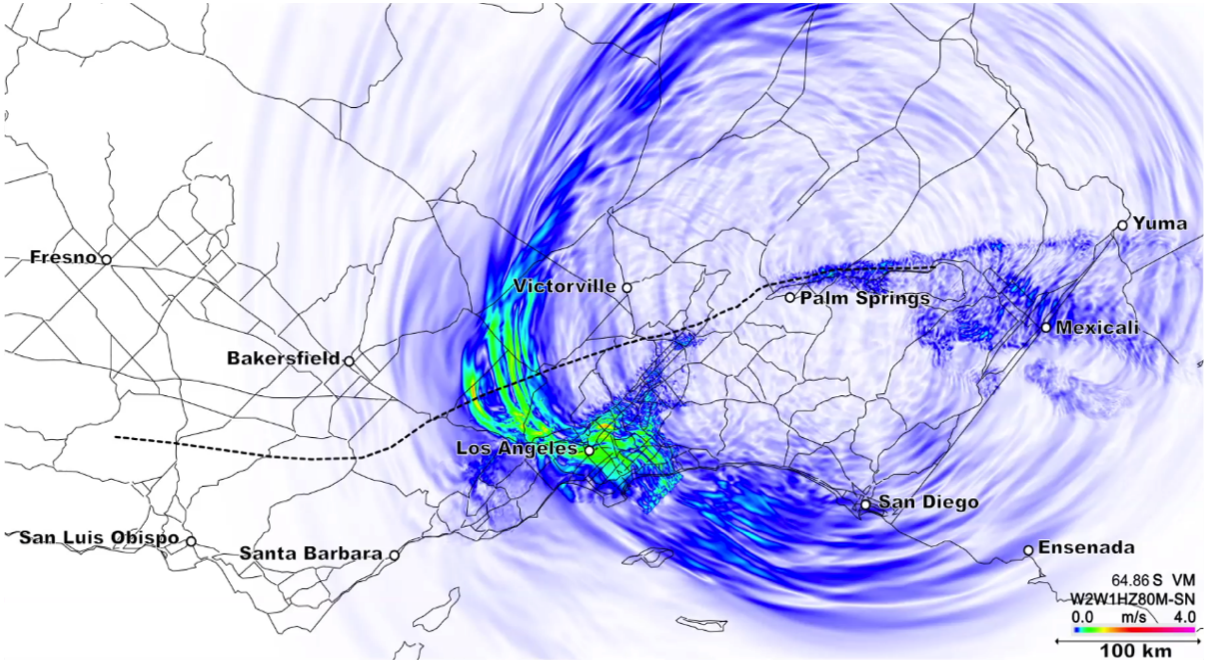

M8 dynamic rupture simulation to study the impact of the rupture direction on peak ground motions in Southern California (2010, SCEC)

The high-frequency challenge

- What do we need to model the observed incoherent high frequency seismic wave field?

  >1 Hz: resonance frequencies of man-made structures

  ~20 Hz: content of broadband ground motion data

$$v = \lambda \cdot f$$

- Limited by lowest shear-wave velocity (available computational resources), knowledge of Earth's structure

- What are the relevant physics at the relevant scales?

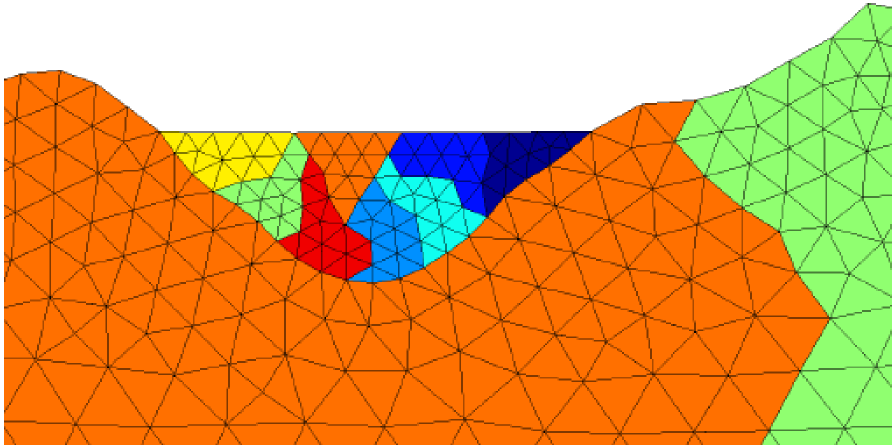

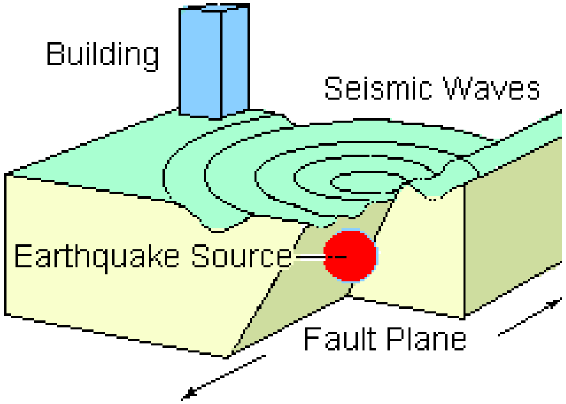

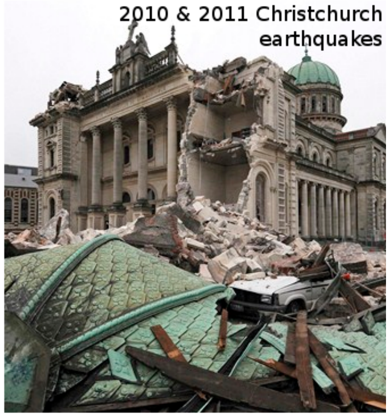

The high-frequency challenge

- What do we need to model the observed incoherent high frequency seismic wave field? Representation of complexities …

→ Earthquake source

Geometry?

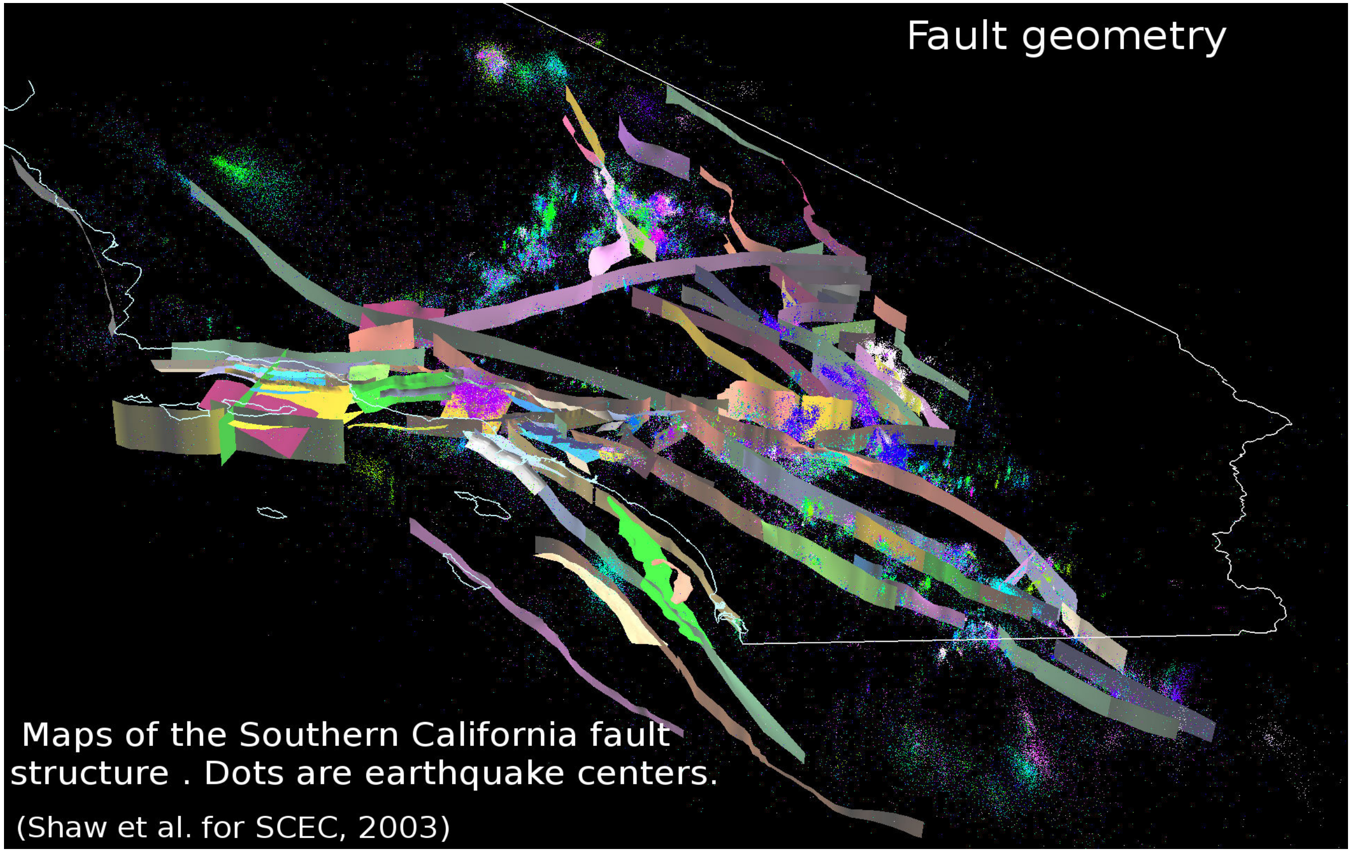

Maps of the Southern California fault structure . Dots are earthquake centers.

(Shaw et al. for SCEC, 2003)

The high-frequency challenge

- What do we need to model the observed incoherent high frequency seismic wave field? Representation of complexities …

→ Earthquake source

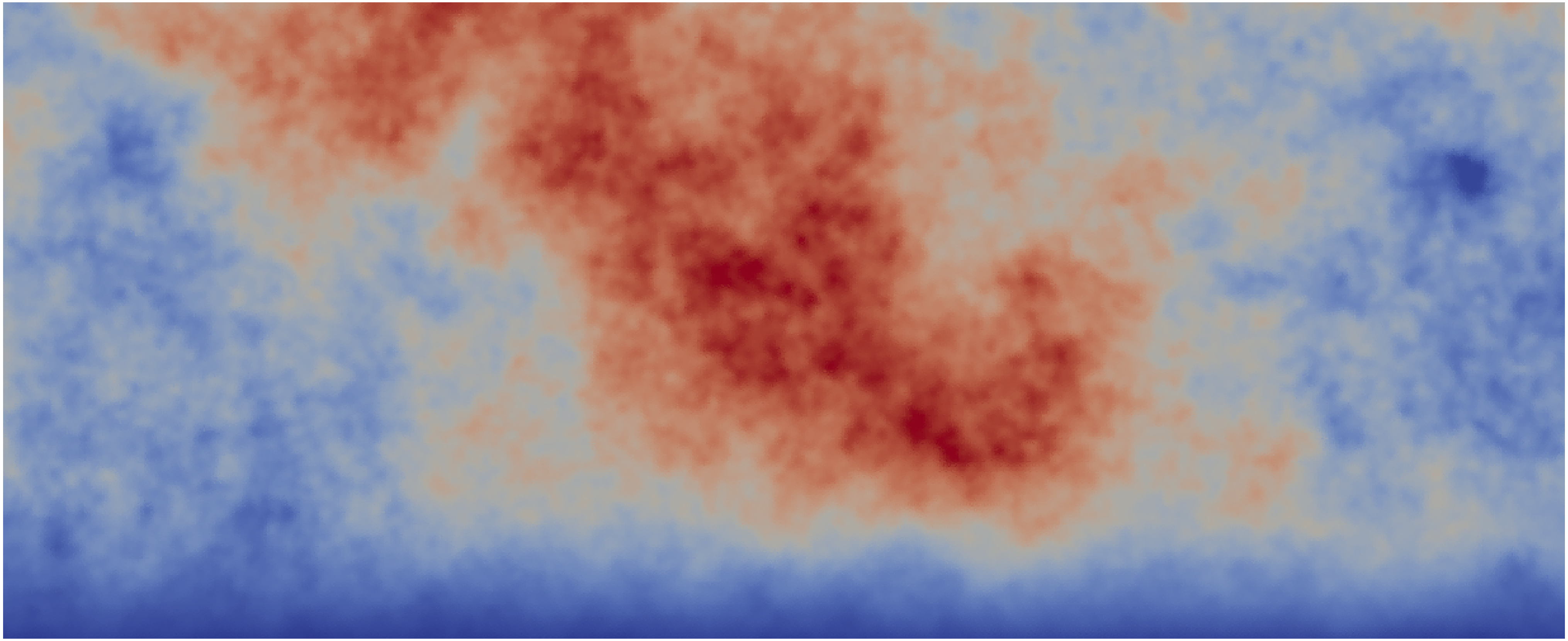

Initial shear stress

The high-frequency challenge

- What do we need to model the observed incoherent high frequency seismic wave field? Representation of complexities …

  - Earthquake source
  - Topography

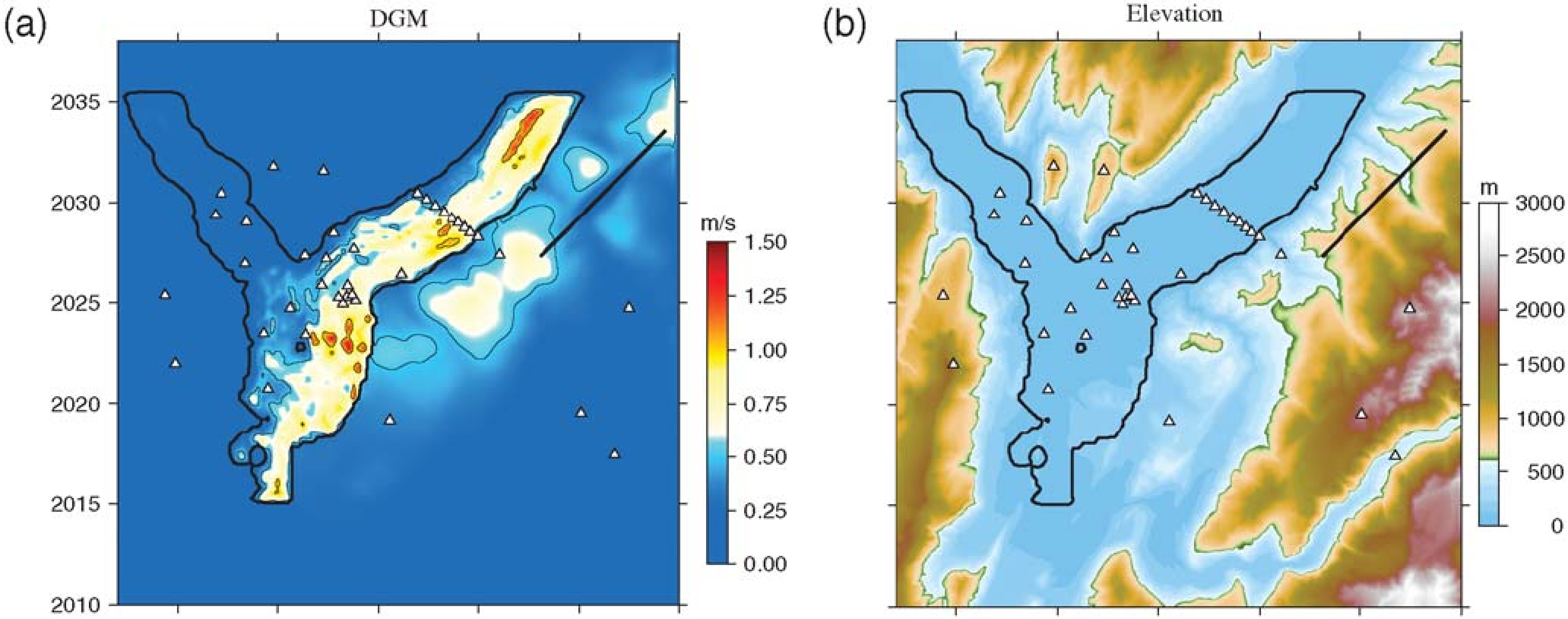

The high-frequency challenge

- What do we need to model the observed incoherent high frequency seismic wave field? Representation of complexities …

→ Earthquake source

→ Topography

→ Media properties

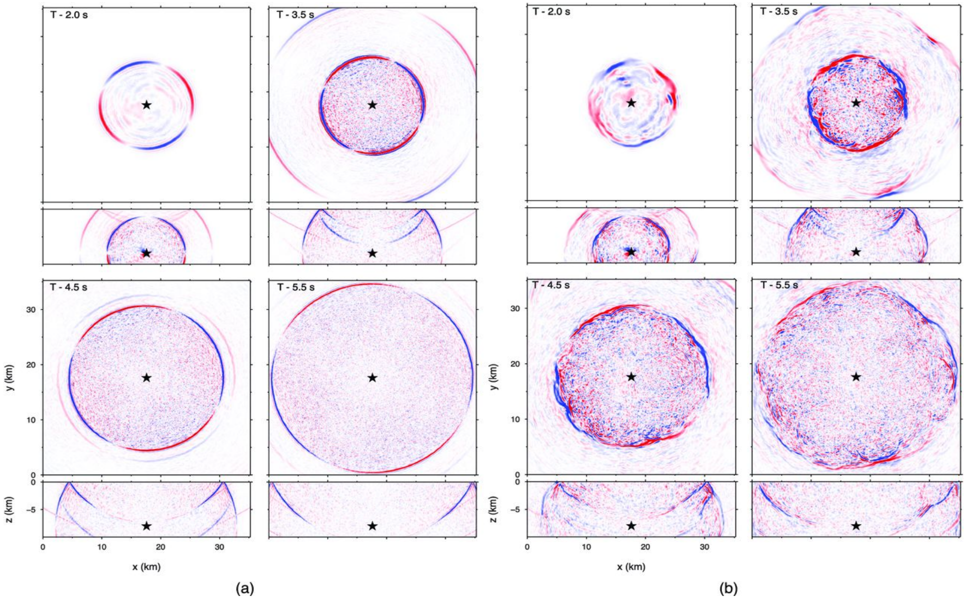

Acceleration field of waves propagating from a point source in heterogeneous random media (Imperatori & Mai, 2013)

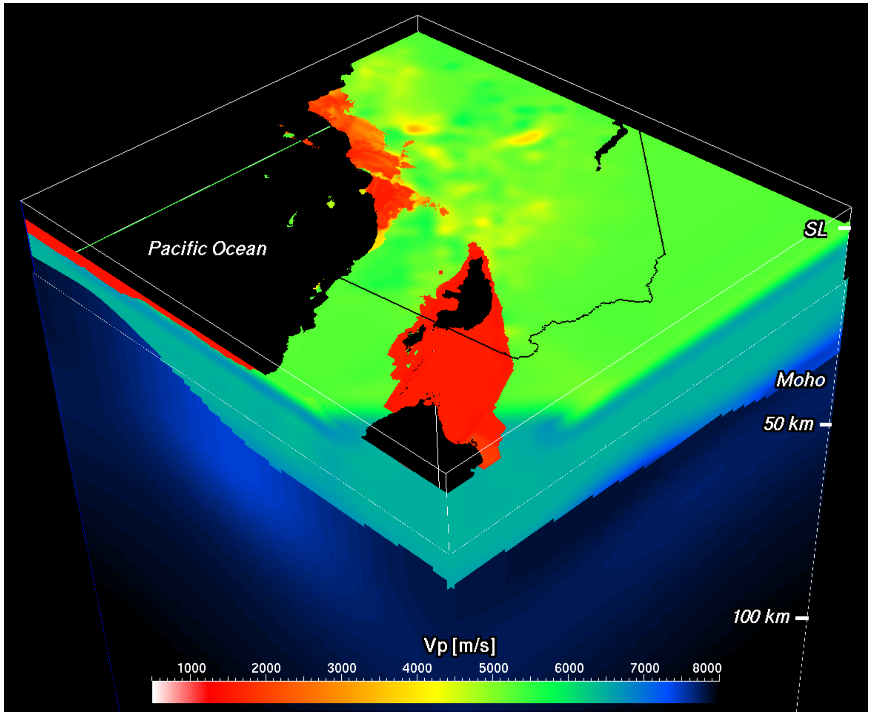

SCEC Community Velocity Model around the Northridge 1994 Earthquake (Mai et al., 2013)

→ Implement complexity in numerical simulations

Long term goal

USGS - http://earthquake.usgs.gov/earthquakes/shakemap/
(modified)

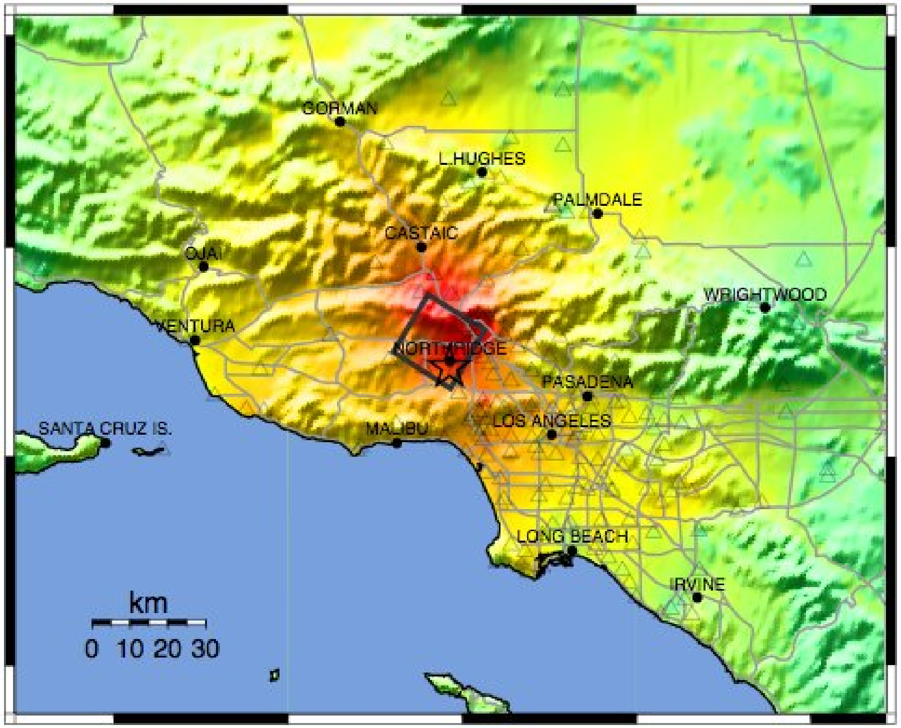

Warmer colors
= higher intensity

Recorded ground motions of the 1994 Northridge Earthquake.

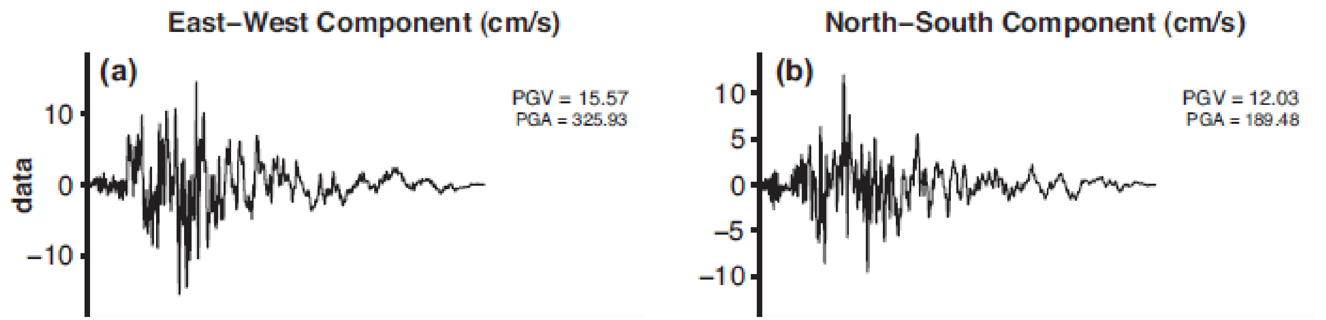

Advantages of the ADER-DG Method

- Enables use of unstructured meshes – low velocity basins, curved or kinked faults, branching, surface rupture, fault interaction
- Mesh coarsening – adjustment of resolution
- High-order accurate simulation of the wave propagation including heterogeneous media and topography
- Local time stepping

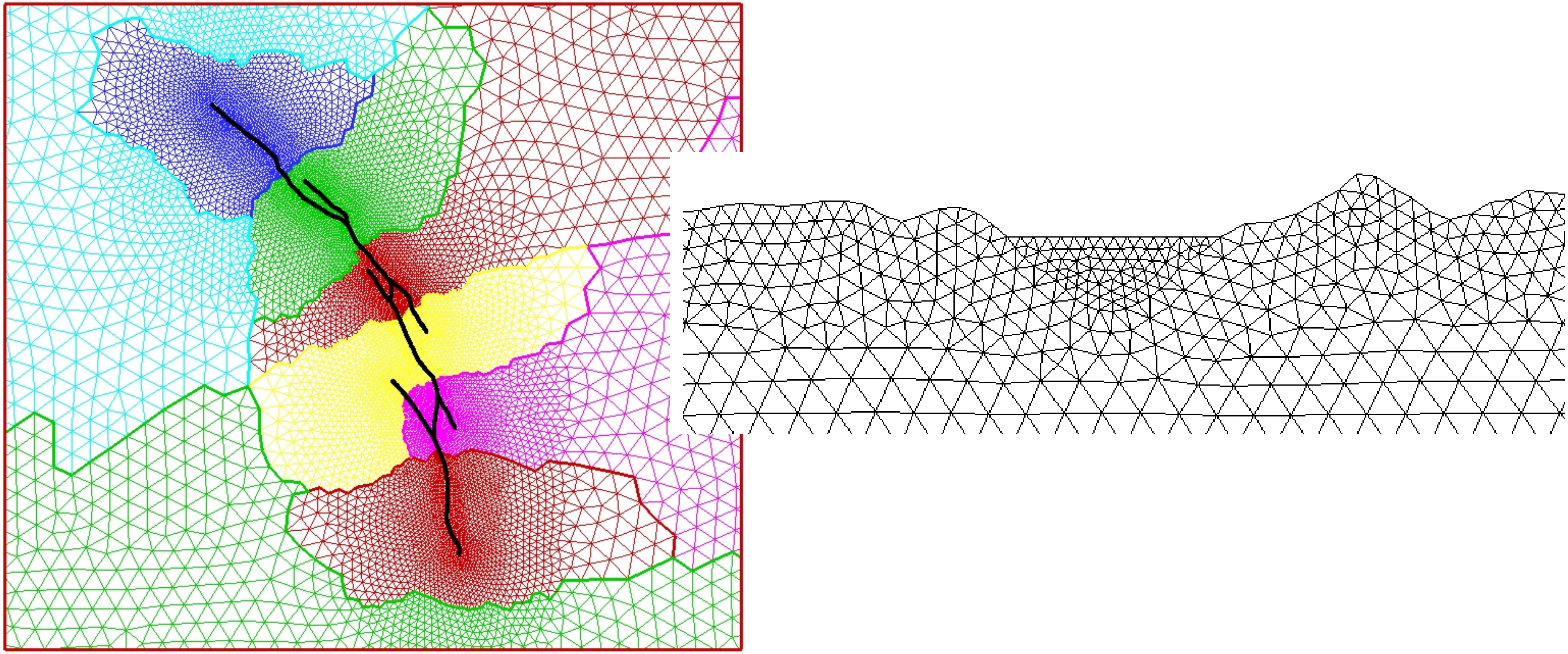

Elastic Wave Equation as a Linear Hyperbolic System:

Vector-matrix notation:

$$\frac{\partial Q_p}{\partial t} + A_{pq}\frac{\partial Q_q}{\partial x} + B_{pq}\frac{\partial Q_q}{\partial y} + C_{pq}\frac{\partial Q_q}{\partial z} = S_p$$

Velocity-stress formulation:

3D: $Q = (\sigma_{xx}, \sigma_{yy}, \sigma_{zz}, \sigma_{xy}, \sigma_{yz}, \sigma_{xz}, u, v, w)^T$

Mathematical Model

Elastic Wave Equation as a Linear Hyperbolic System:

Vector-matrix notation:

$$\frac{\partial Q_p}{\partial t} + A_{pq}\frac{\partial Q_q}{\partial x} + B_{pq}\frac{\partial Q_q}{\partial y} + C_{pq}\frac{\partial Q_q}{\partial z} = S_p$$

Velocity-stress formulation:

3D: $Q = (\sigma_{xx}, \sigma_{yy}, \sigma_{zz}, \sigma_{xy}, \sigma_{yz}, \sigma_{xz}, u, v, w)^T$

Numerical Approximation of the solution

$$\left(Q_h^{(m)}\right)_p(\xi,\eta,\zeta,t) = \hat{Q}_{pl}^{(m)}(t)\Phi_l(\xi,\eta,\zeta)$$

- Φ_l are orthogonal basis functions
- the mass matrix is diagonal

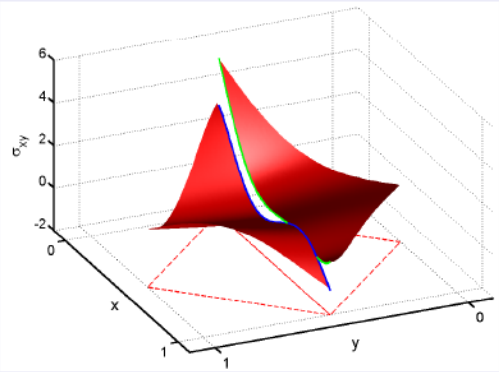

(Fig. from de la Puente et al., 2009)

Semi-discrete form of the scheme

Multiply by testfunction Φ_l and integrate over element $\mathcal{T}^{(m)}$:

$$\int_{\mathcal{T}^{(m)}} \Phi_k \frac{\partial Q_p}{\partial t} dV + \int_{\mathcal{T}^{(m)}} \Phi_k \left(A_{pq} \frac{\partial Q_q}{\partial x} + B_{pq} \frac{\partial Q_q}{\partial y} + C_{pq} \frac{\partial Q_q}{\partial z} \right) dV = \int_{\mathcal{T}^{(m)}} \Phi_k S_p dV$$

Integrate second term by parts:

$$\int_{\partial \mathcal{T}^{(m)}} \Phi_k F_p dS - \int_{\mathcal{T}^{(m)}} \left(\frac{\partial \Phi_k}{\partial x} A_{pq} Q_q + \frac{\partial \Phi_k}{\partial y} B_{pq} Q_q + \frac{\partial \Phi_k}{\partial z} C_{pq} Q_q \right) dV$$

Flux term:

$$\int_{\partial \mathcal{T}} \Phi_k F_p dS = \sum_{j=1}^{\# \, sides} \int_0^1 \Phi_k F_p^{(j)} \left| S_j \right| dS$$

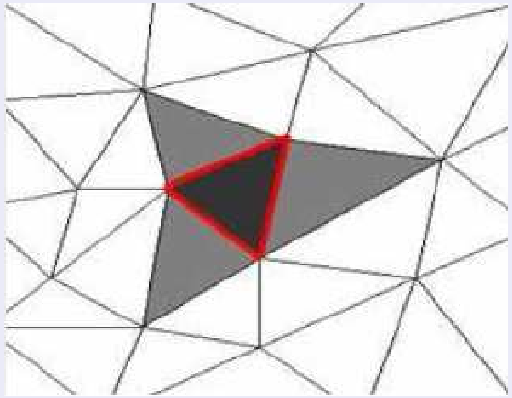

Discontinuous Galerkin Approach – Flux computation

Flux computation

Exact Riemann solver is used to compute the state at the interfaces by upwinding:

$$
\begin{aligned}
F_p^h &= \frac{1}{2} T_{pq} \left(A_{qr}^{(m)} + \left| A_{qr}^{(m)} \right| \right) (T_{rs})^{-1} \hat{Q}_{sl}^{(m)} \Phi_l^{(m)} \\
&+ \frac{1}{2} T_{pq} \left(A_{qr}^{(m)} - \left| A_{qr}^{(m)} \right| \right) (T_{rs})^{-1} \hat{Q}_{sl}^{(m_j)} \Phi_l^{(m_j)}
\end{aligned}
$$

Locality of the computations:
only directly neighboring elements are required to exchange data, which leads to small communication times for parallel calculations

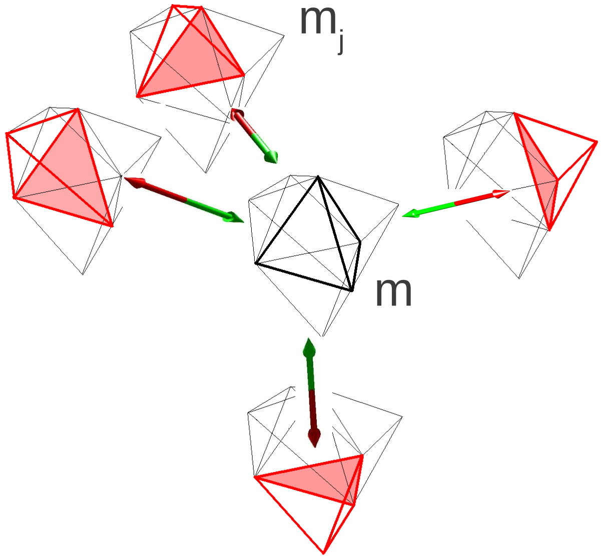

Suitability for large scale HPC infrastructure

Efficiency on the BlueGene/P machine Shaheen at KAUST

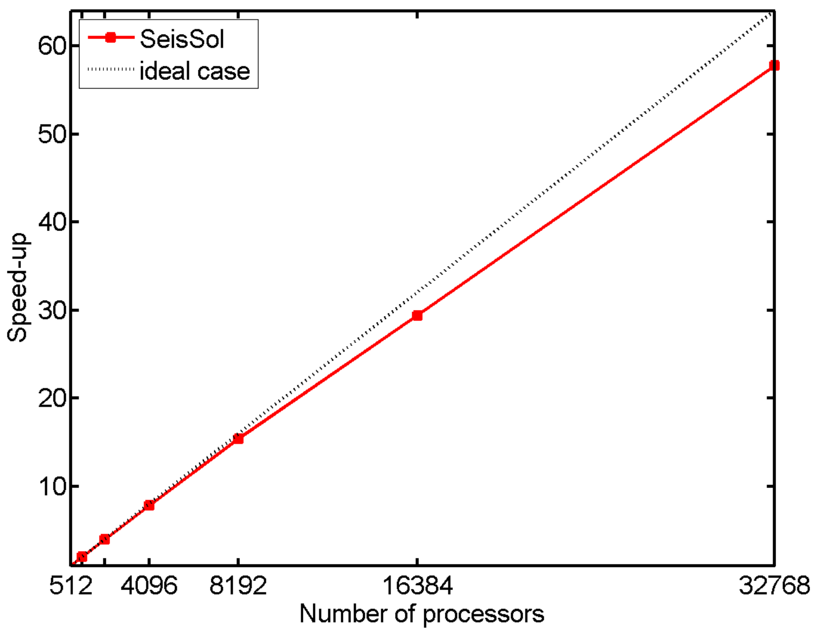

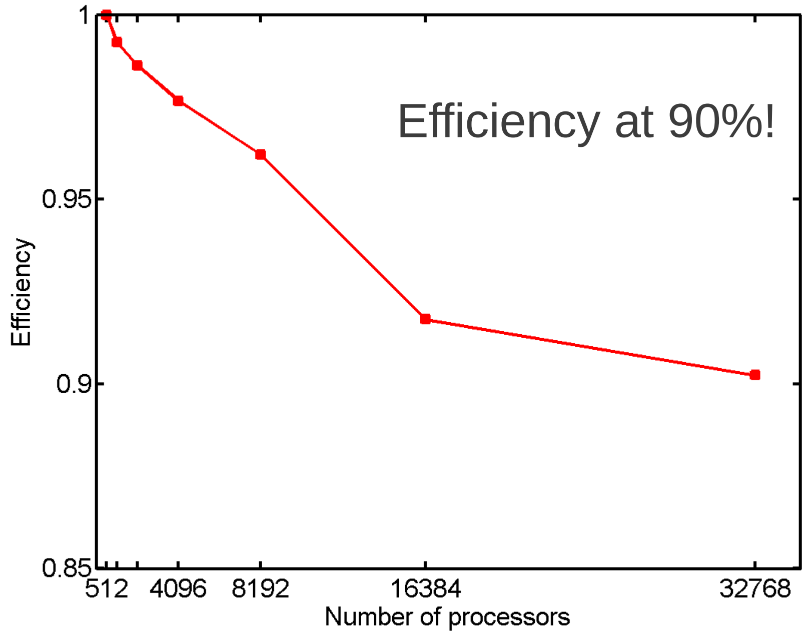

- 7,7 Mio. Elements
- Order of accuracy in space and time: O5
- Pure MPI parallelization – code is openMP hybrid now
- Metis partitioning

  http://glaros.dtc.umn.edu/gkhome/metis/metis/overview

ADER time integration

Cauchy-Kovalewski procedure

Taylor expansion:

$$\begin{aligned} Q_p(\xi,\eta,\zeta,t) &= \sum_{k=0}^{N} \frac{t^k}{k!}\frac{\partial^k}{\partial t^k} Q_p(\xi,\eta,\zeta,0) \\ &= \sum_{k=0}^{N} \frac{t^k}{k!}(-1)^k \left(A^*_{pq}\frac{\partial}{\partial \xi} + B^*_{pq}\frac{\partial}{\partial \eta} + C^*_{pq}\frac{\partial}{\partial \zeta} \right)^k \Phi_l \hat{Q}_{ql}(0) \end{aligned}$$

Projection onto basis function and integration over one timestep:

$$\int_{t_n}^{t_{n+1}} \hat{Q}_{pl}(\tau) d\tau = \ldots$$

Only one time step has to be kept in memory!

ADER time integration – Local time stepping

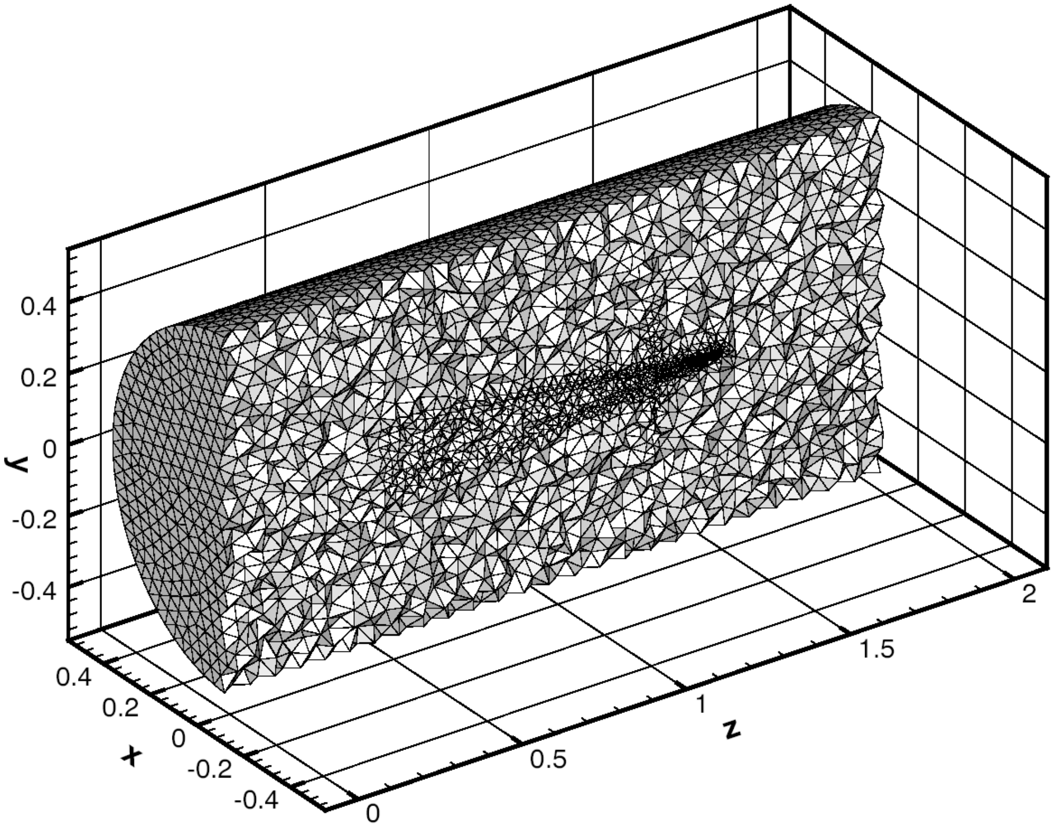

← Example:
Stiff inclusion
(modified after LeVeque 2002)

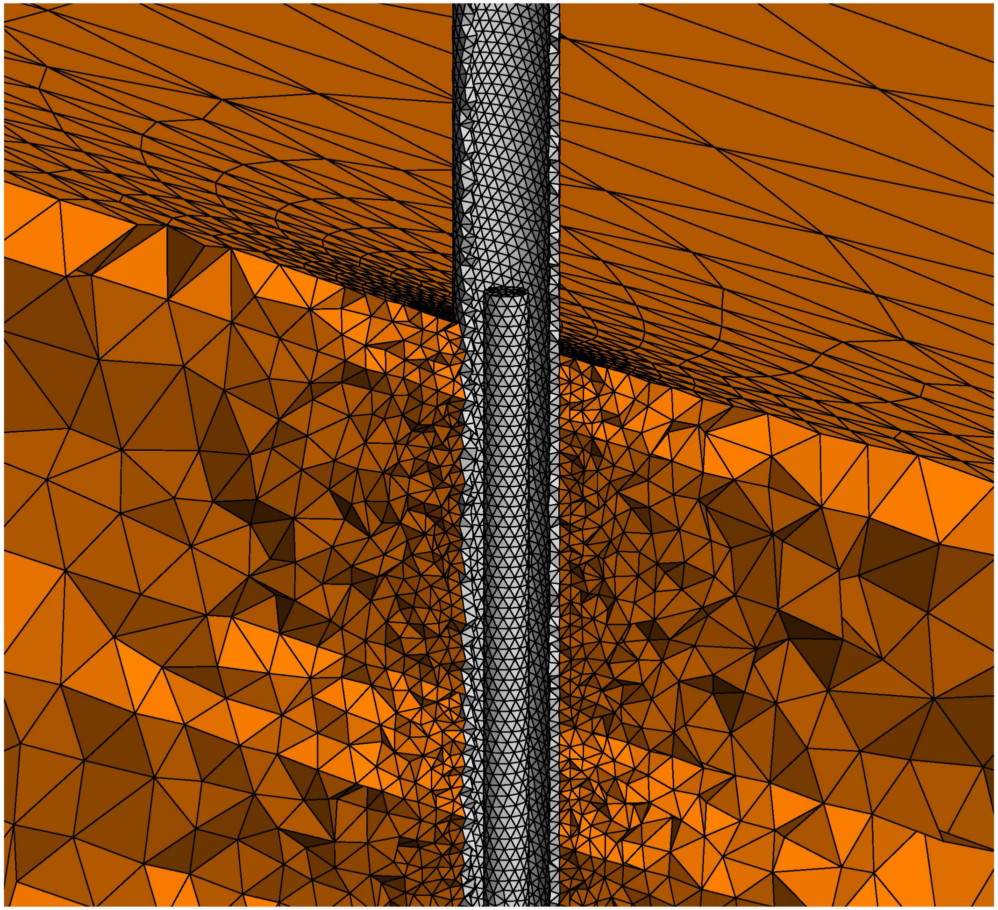

Number of element-updates:

- 72 *10^9 with <u>global</u> time step
- 95 *10^7 with <u>local</u> time step

Speedup: ~100!

ADER time integration – Local time stepping

Load balancing? → Clustered LTS!

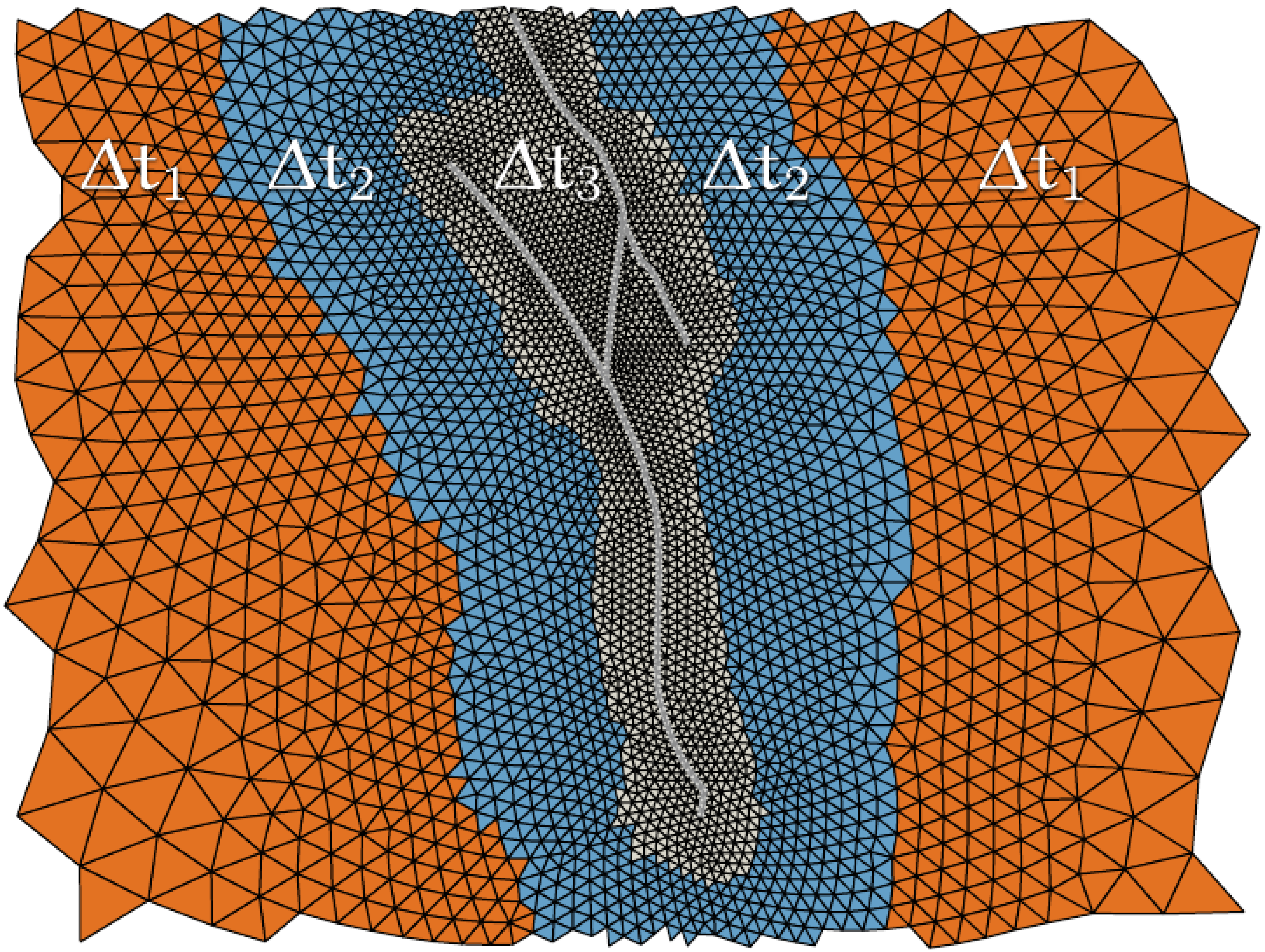

Image by A. Breuer

Dynamic Earthquake rupture

Incorporate source process

- To understand earthquake faulting
- Support physics-based ground motion prediction

Treat dynamic rupture as an interior time-dependent 'boundary condition' using the flux term!

- Impose new traction following the failure criterion
- Impose fault parallel velocities in opposite directions

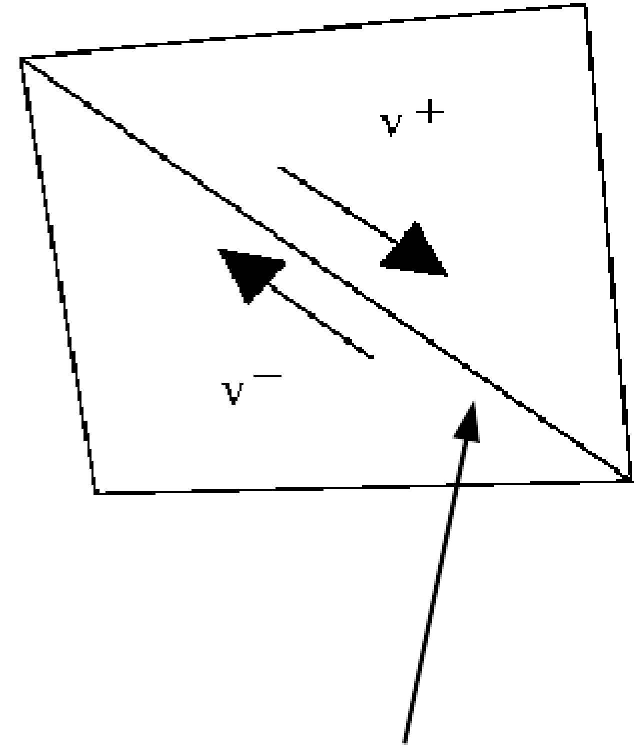

fault between
two elements

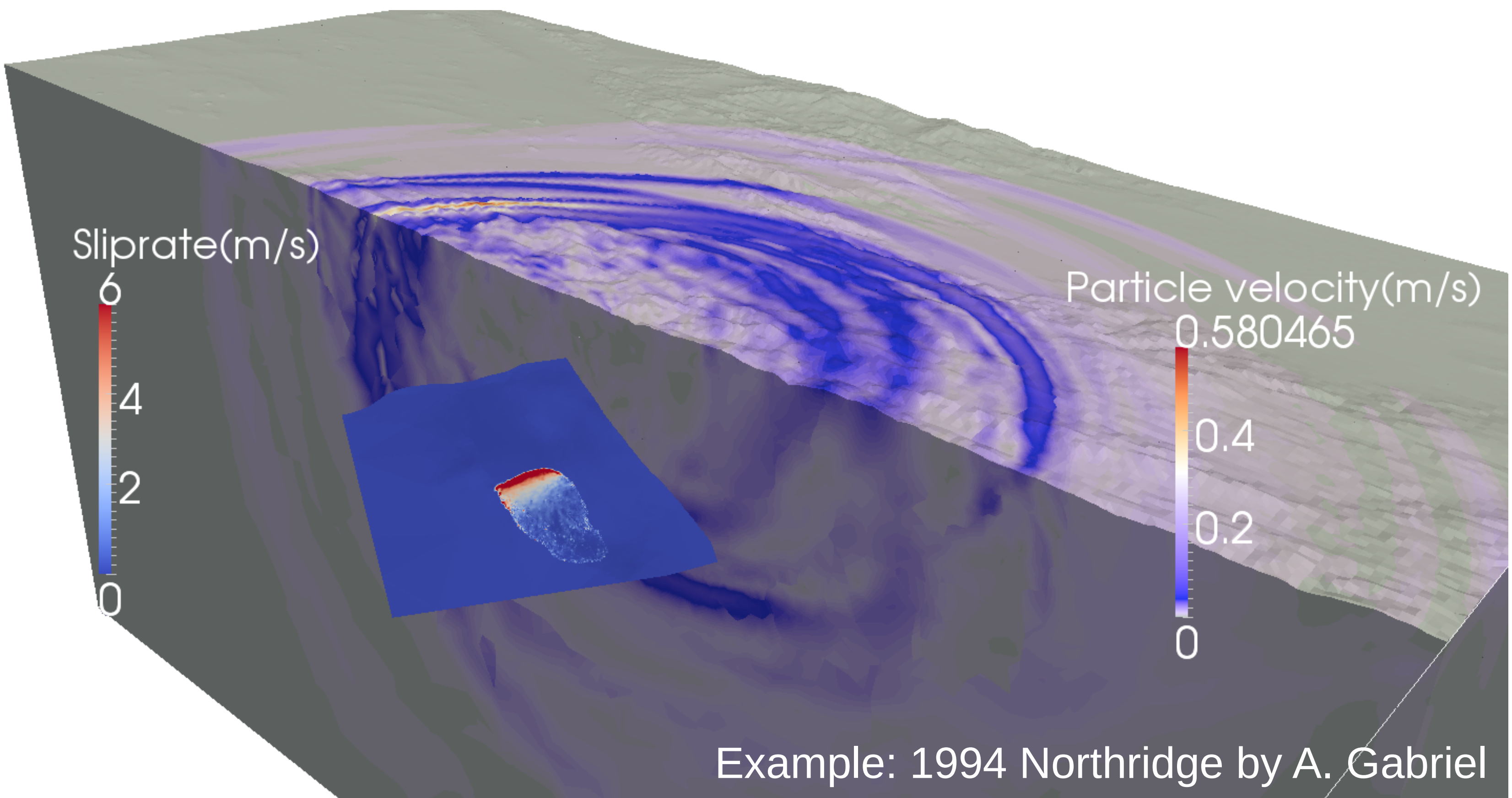

Ingredients

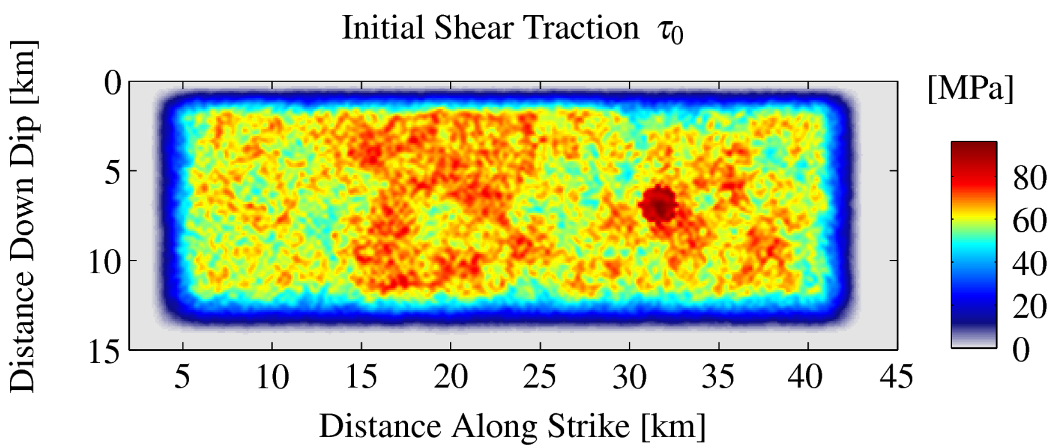

(Brietzke et al. (2009))

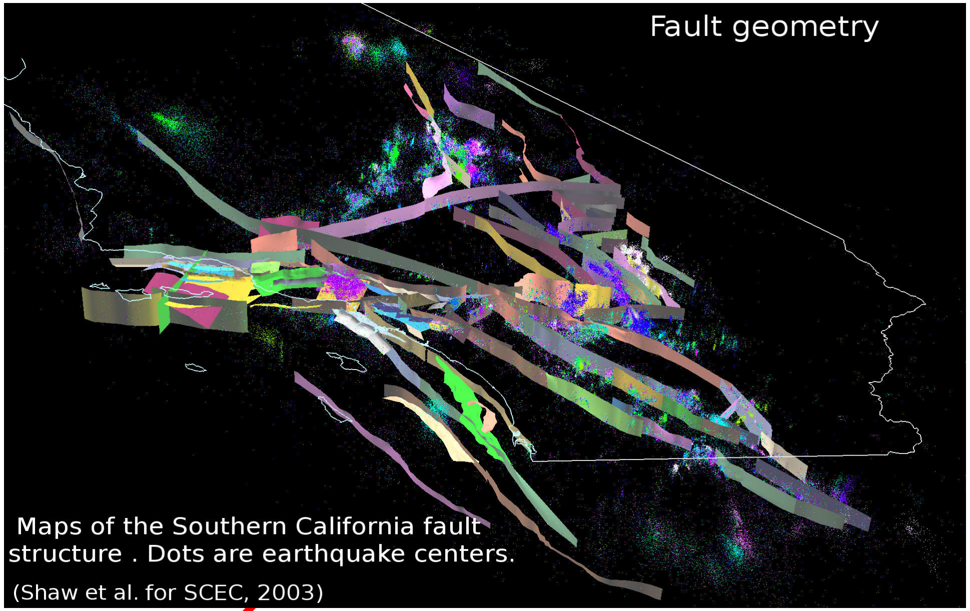

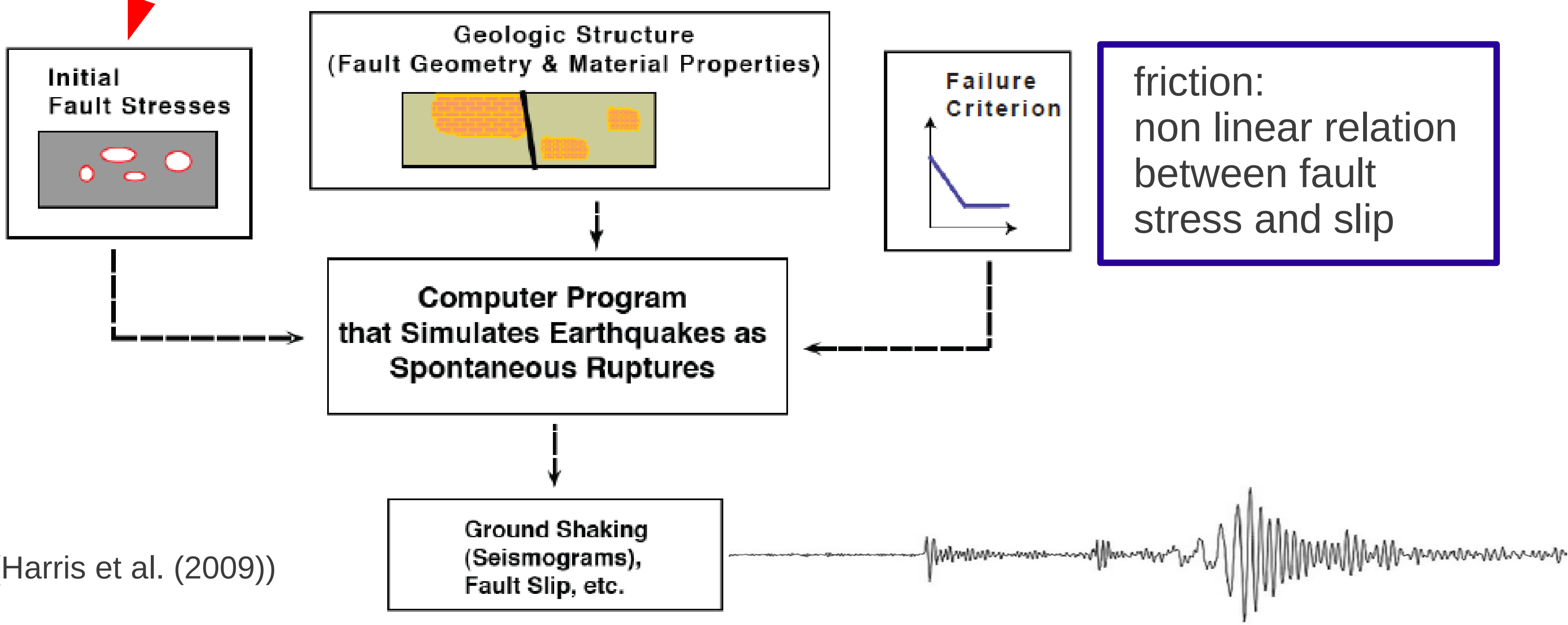

friction:
non linear relation between fault stress and slip

(Harris et al. (2009))

Failure criterion:

Coulomb friction model

$$\underbrace{|\sigma_{xy}|}_{\text{traction}} \le \underbrace{\mu_f \sigma}_{\text{fault strength}}$$

$$(|\sigma_{xy}| - \mu_f \sigma)\Delta v = 0$$

σ_{xy} traction

μ_f friction coefficient

σ normal stress

Δv slip rate

Failure criterion:

Coulomb friction model

$$|\sigma_{xy}| \leq \mu_f \sigma$$

traction   fault strength

$$(|\sigma_{xy}| - \mu_f \sigma)\Delta v = 0$$

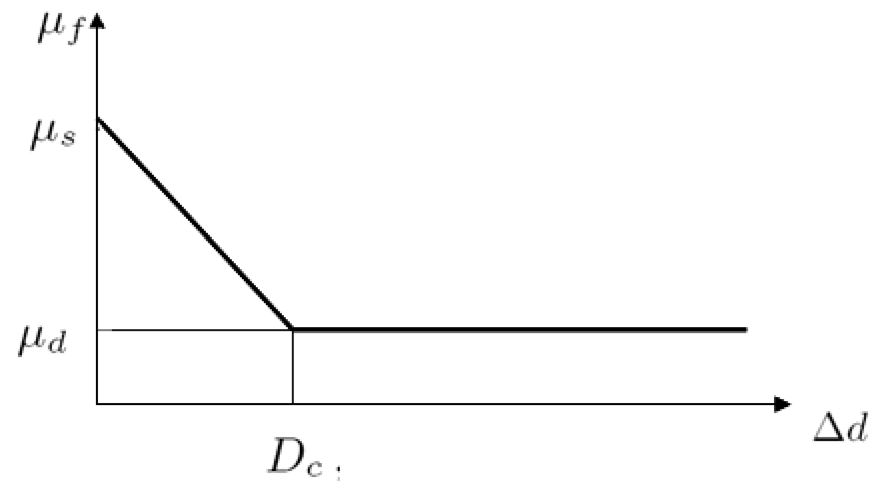

σ_{xy} traction

μ_f friction coefficient

σ normal stress

Δv slip rate

Δd slip

D_c critical slip distance

Linear Slip Weakening friction law
(laboratory experiments
– rate-and-state also implemented)

Provides:

- initial rupture
- arrest of sliding
- reactivation of slip

Comparison SpecFEM and ADER-DG: TPV5

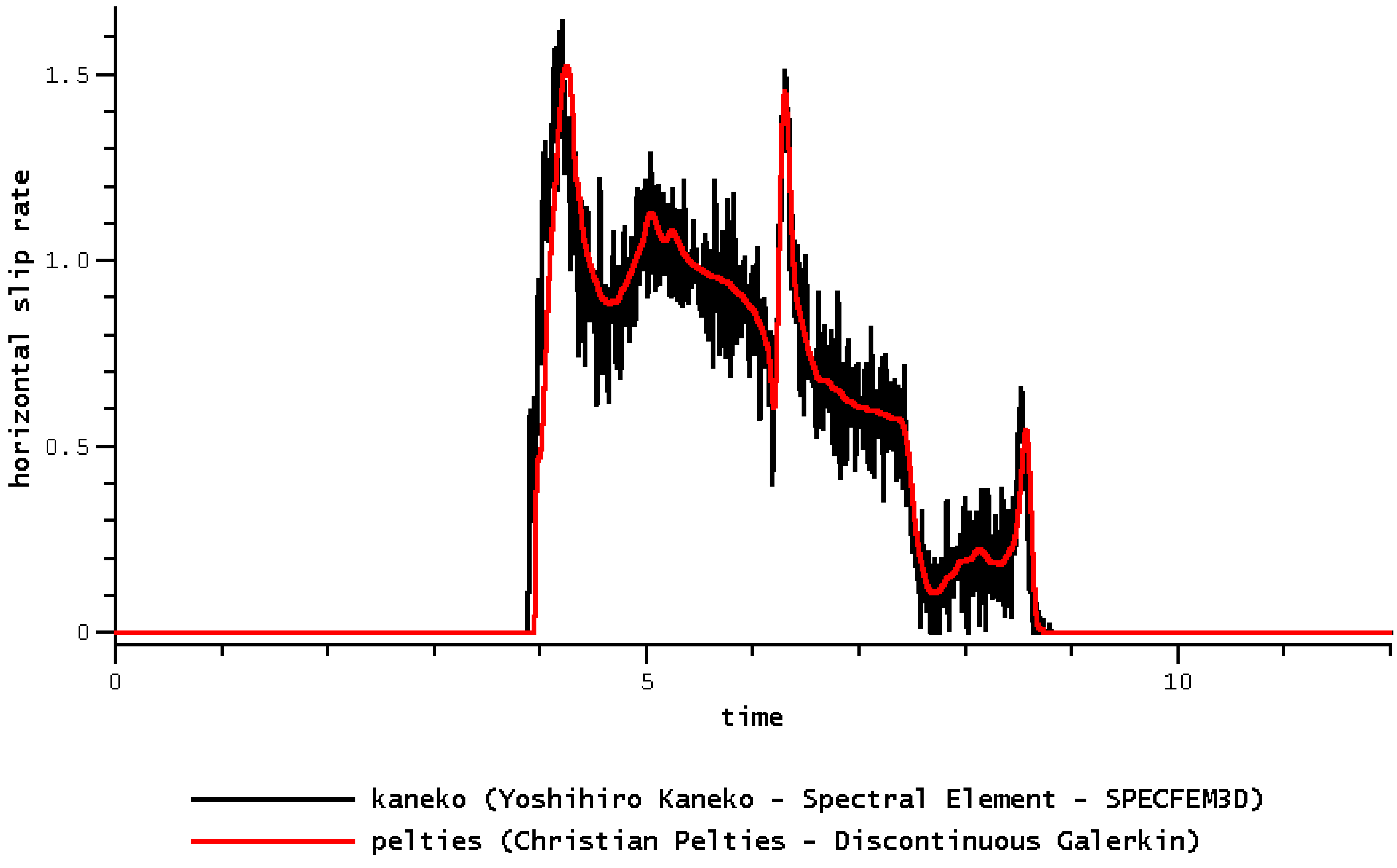

Visualization

- Wavefield and Dynamic Rupture
  - Interpretation of results
  - Clear communication to non-experts

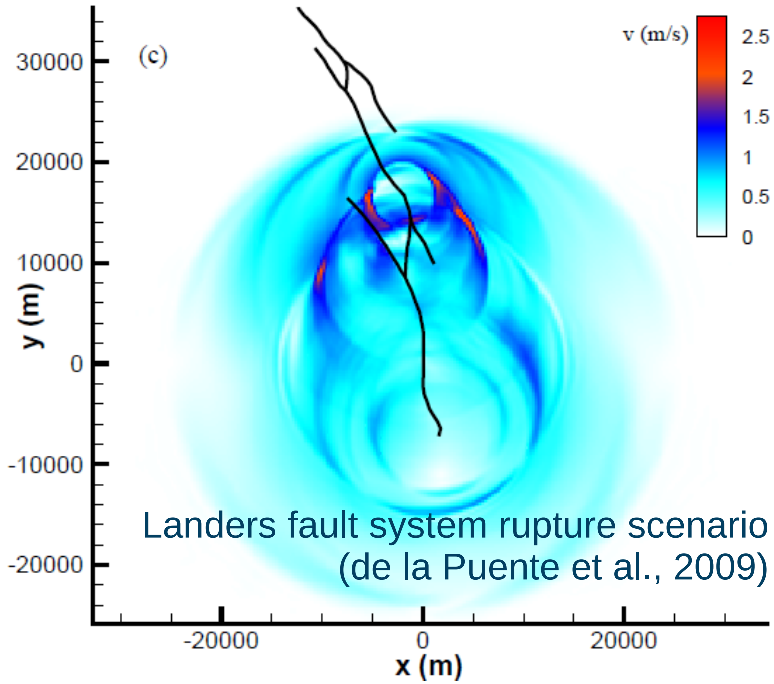

Landers fault system rupture scenario (de la Puente et al., 2009)

- Challenges
  - Scalable with minimal impact on performance
  - Full output of DOFs too large
  - Appropriate means to sample data on unstructured meshes

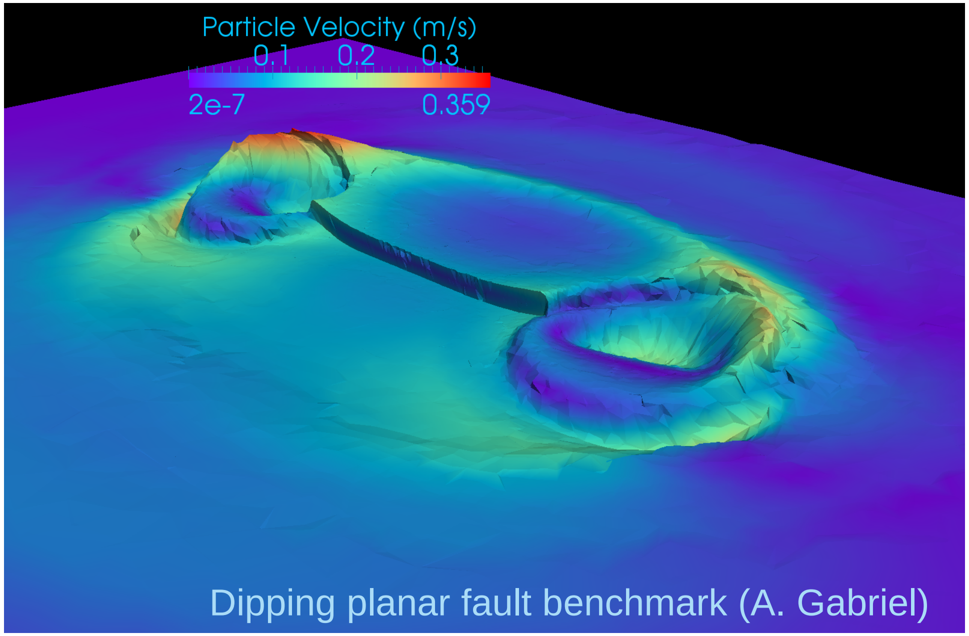

Dipping planar fault benchmark (A. Gabriel)

Visualization

- Wavefield and Dynamic Rupture Visualization with HDF5 + ParaView
  - Binary, parallel I/O for unstructured meshes
  - Flexibility regarding the type of data
  - Reduction of data by a factor of ~4 - 8 compared to ASCII Tecplot
  - Recursive sub-tetrahedral sampling

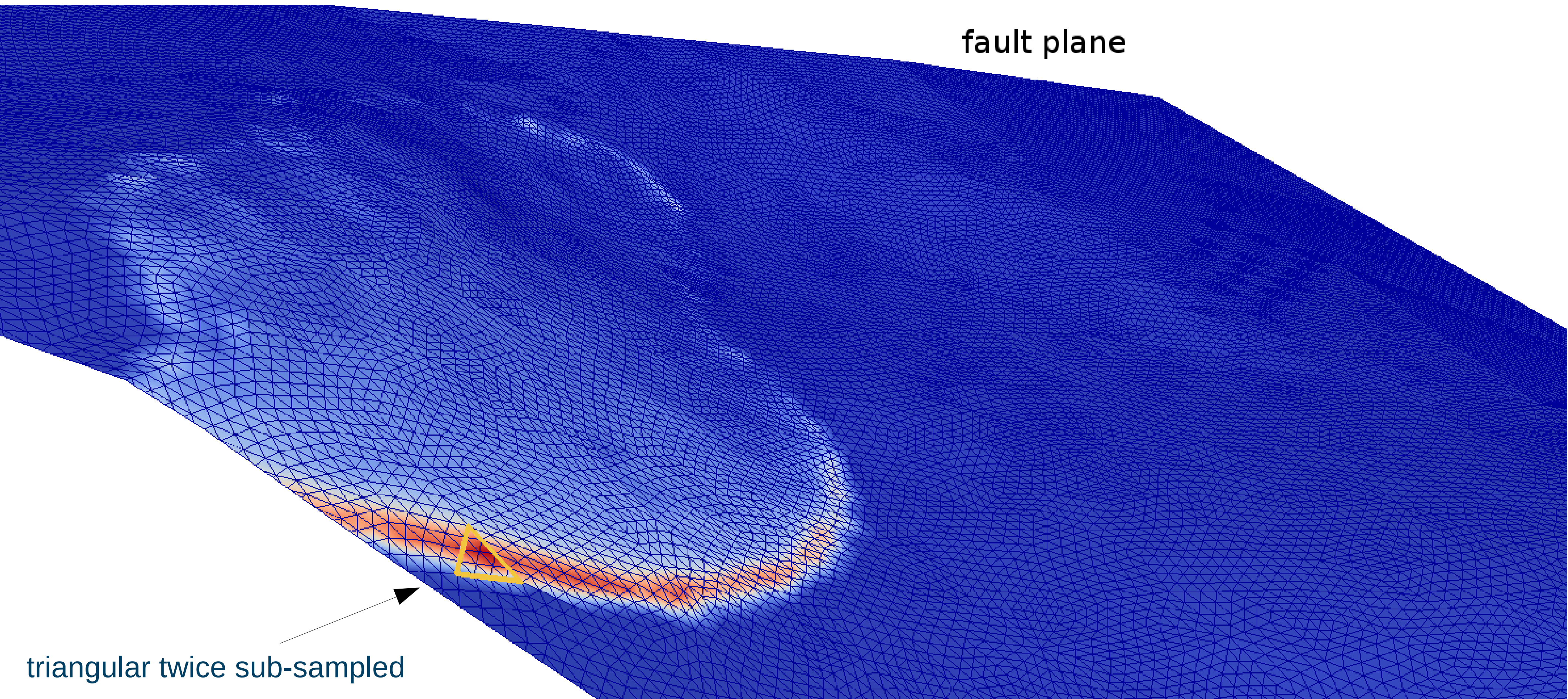

Kernel optimization

Problem

- ~75% of the runtime is consumed by small sparse matrix-matrix multiplications
- Available libraries (sparse or dense) only with minor improvements

Solution

- Write optimal code on hardware level
- Explicit vectorization of element-local operations

Contribution of TUM group within ASCETE - Thanks to Alex Breuer for providing the figures!

Kernel optimization

Example: CK-Procedure

Time derivatives are defined as a recursive scheme with $\frac{\partial^0}{\partial t^0} Q_k = Q_k^n$

$$\frac{\partial^{j+1}}{\partial t^{j+1}} Q_k = -M^{-1} \left((K^\xi)^T \left(\frac{\partial^j}{\partial t^j} Q_k \right) A_k^* + (K^\eta)^T \left(\frac{\partial^j}{\partial t^j} Q_k \right) B_k^* + (K^\zeta)^T \left(\frac{\partial^j}{\partial t^j} Q_k \right) C_k^* \right)$$

$$(K^\zeta)^T \qquad \frac{\partial^j}{\partial t^j} Q_k \qquad C_k^*$$

Resulting into the sparsity patterns of an order 5 scheme:

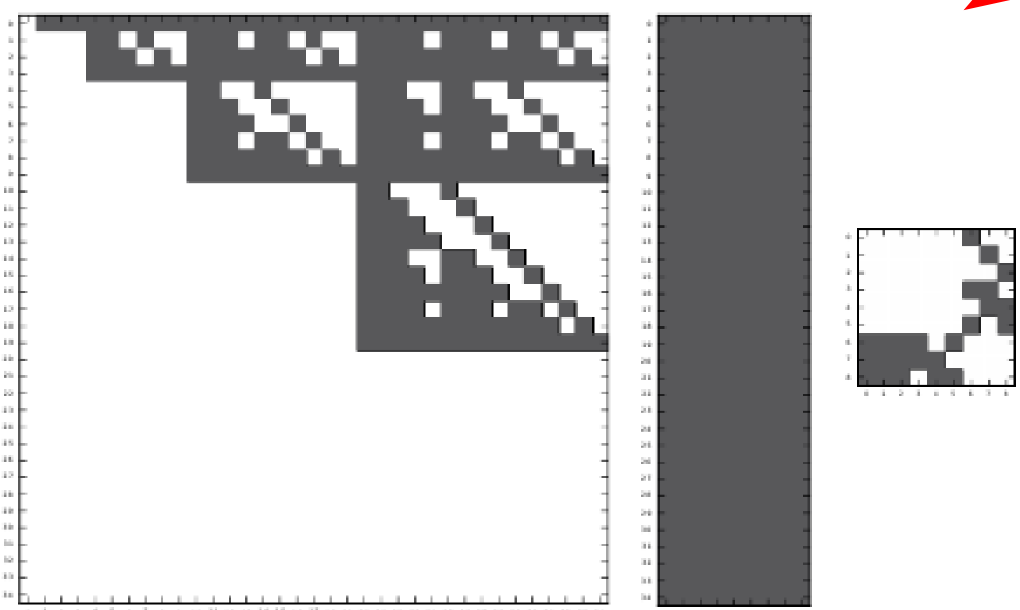

Kernel optimization

Example: CK-Procedure

Memory layout

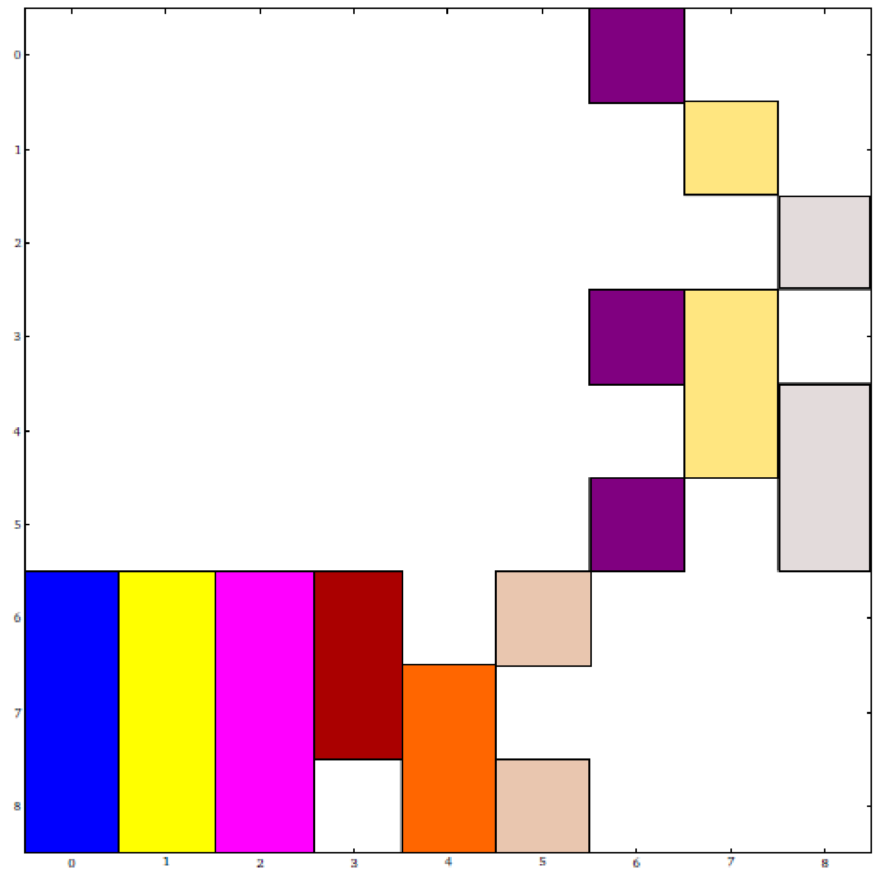

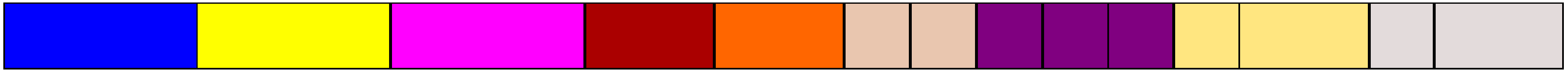

Kernel optimization

Example: CK-Procedure

'intrinsics'

'loop unrolling'

```
#if defined(__SSE3__) && defined(__AVX256__)
__m256d c3_0 = _mm256_loadu_pd(&C[(i*10)+4]);
__m256d a3_0 = _mm256_loadu_pd(&values[16]);
c3_0 = _mm256_add_pd(c3_0, _mm256_mul_pd(a3_0, b3));
_mm256_storeu_pd(&C[(i*10)+4], c3_0);
#endif
#if defined(__SSE3__) && !defined(__AVX256__)
__m128d c3_0 = _mm_loadu_pd(&C[(i*10)+4]);
__m128d a3_0 = _mm_loadu_pd(&values[16]);
c3_0 = _mm_add_pd(c3_0, _mm_mul_pd(a3_0, b3));
_mm_storeu_pd(&C[(i*10)+4], c3_0);
__m128d c3_2 = _mm_loadu_pd(&C[(i*10)+6]);
__m128d a3_2 = _mm_loadu_pd(&values[18]);
c3_2 = _mm_add_pd(c3_2, _mm_mul_pd(a3_2, b3));
_mm_storeu_pd(&C[(i*10)+6], c3_2);
#endif
__m128d c3_4 = _mm_loadu_pd(&C[(i*10)+8]);
__m128d a3_4 = _mm_loadu_pd(&values[20]);
#if defined(__SSE3__) && defined(__AVX256__)
c3_4 = _mm_add_pd(c3_4, _mm_mul_pd(a3_4, _mm256_castpd256_pd128(b3)));
#endif
#if defined(__SSE3__) && !defined(__AVX256__)
c3_4 = _mm_add_pd(c3_4, _mm_mul_pd(a3_4, b3));
#endif
_mm_storeu_pd(&C[(i*10)+8], c3_4);
#else
C[(i*10)+4] += values[16] * B[(i*10)+3];
C[(i*10)+5] += values[17] * B[(i*10)+3];
C[(i*10)+6] += values[18] * B[(i*10)+3];
C[(i*10)+7] += values[19] * B[(i*10)+3];
C[(i*10)+8] += values[20] * B[(i*10)+3];
C[(i*10)+9] += values[21] * B[(i*10)+3];
#endif
```

Kernel optimization

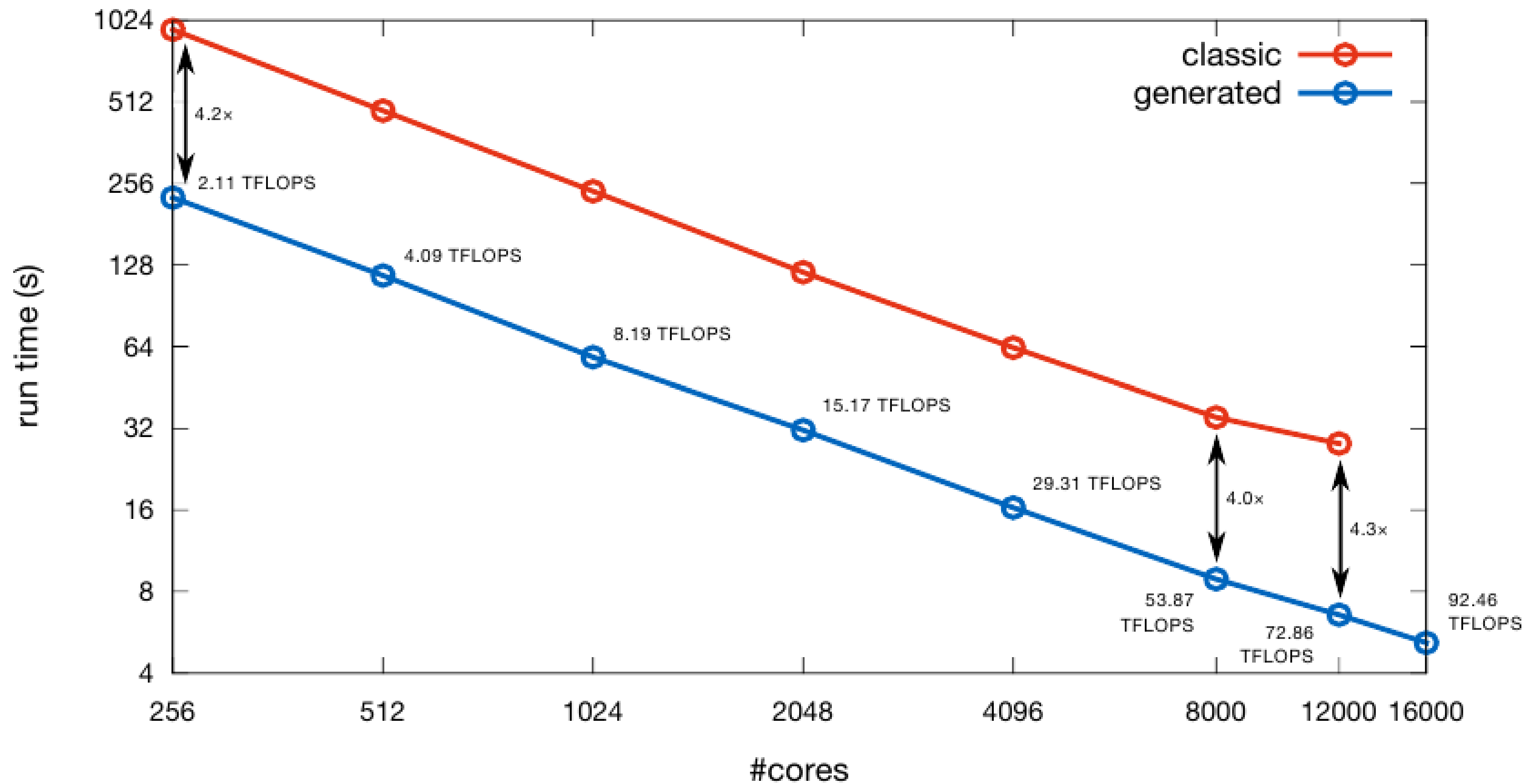

- SuperMUC, LRZ, Germany
- Intel Xeon E5-2680 (SNB-EP) @ 2.7 GHz
- Strong scaling
- 7.25 mio. cells
- 6th order
- Up to ~38% peak performance

Workflow

From CAD to seismogram...

"Time to solution!"

- Get geometry and model data
- Assemble CAD model
- Create mesh
- Partitioning
- Set model parameters
- Solve physical equation
- Analysis of output

Pre-processing

Post-processing

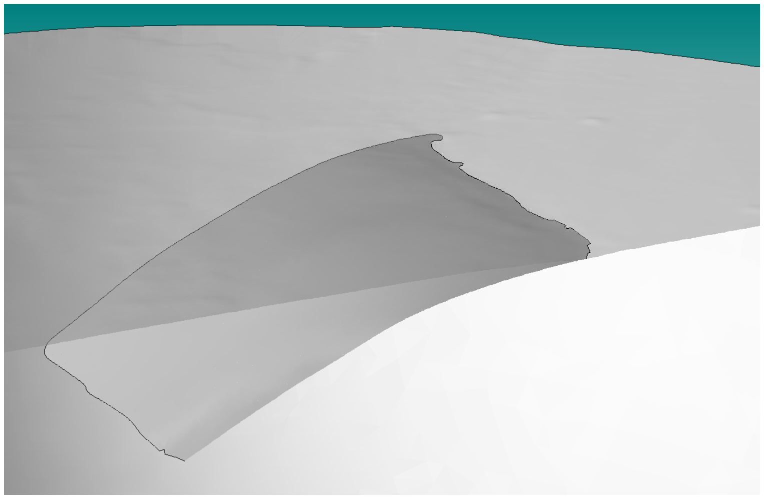

Automated CAD generation

Current bottleneck: CAD generation can easily consume weeks to month

Difficulties:

- Surface reconstruction of different types of initial raw data
- Undulating 3D surfaces that merge under shallow angles, intersect
- Remove non-physical features
- Clip too small features depending on the desired mesh size
- Representation by splines as typically used by (commercial) CAD/mesh software unfortunate for geological data
- Watertight model
- Seamless integration into meshing software (avoid format conversion)

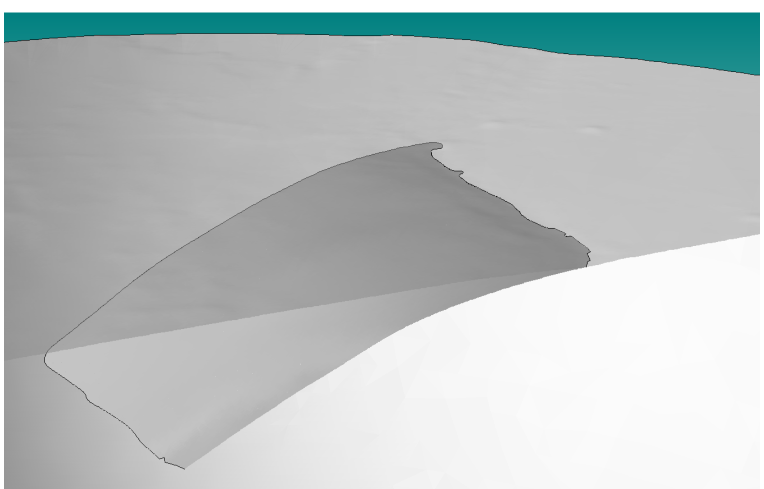

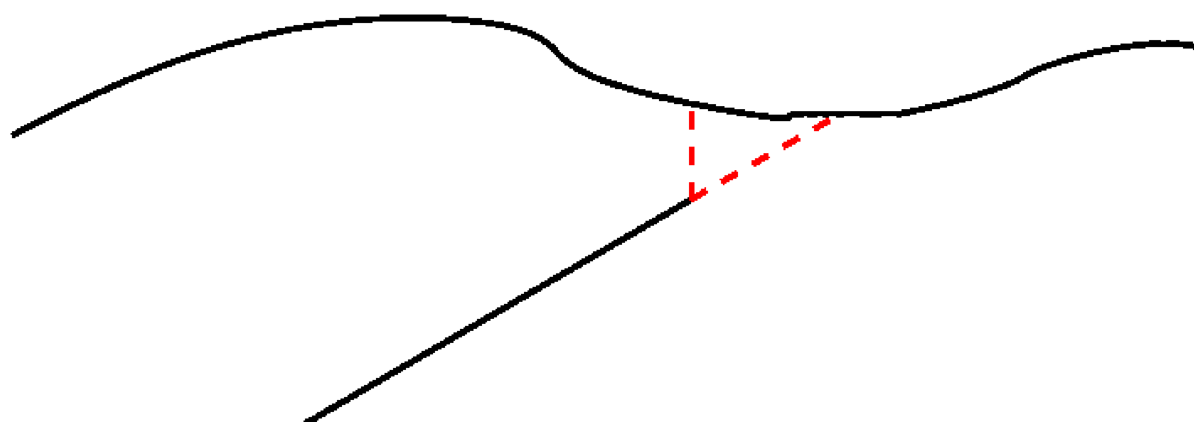

SimModeler

Customized problem definition and mesh generation interface for SeisSol
by **RPI/SCOREC/Simmetrix (C. Smith, M. Shephard)**

- Mesh coarsening/refining
- Handling complex geometries
- user-friendly interface
- Quality metrics
- Exports SeisSol format
- Non-manifold geometry required

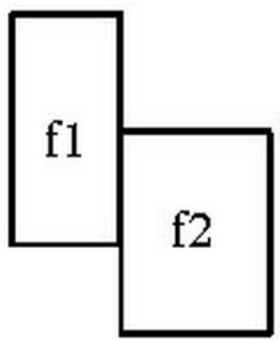

Two faces. At the intersection there are two edges overlapping.
= assembly

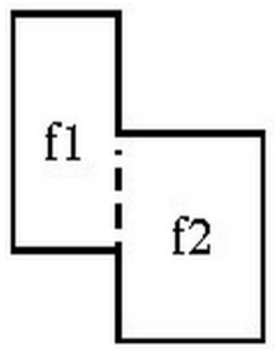

Two faces. At the intersection there is one shared edge.
= non-manifold

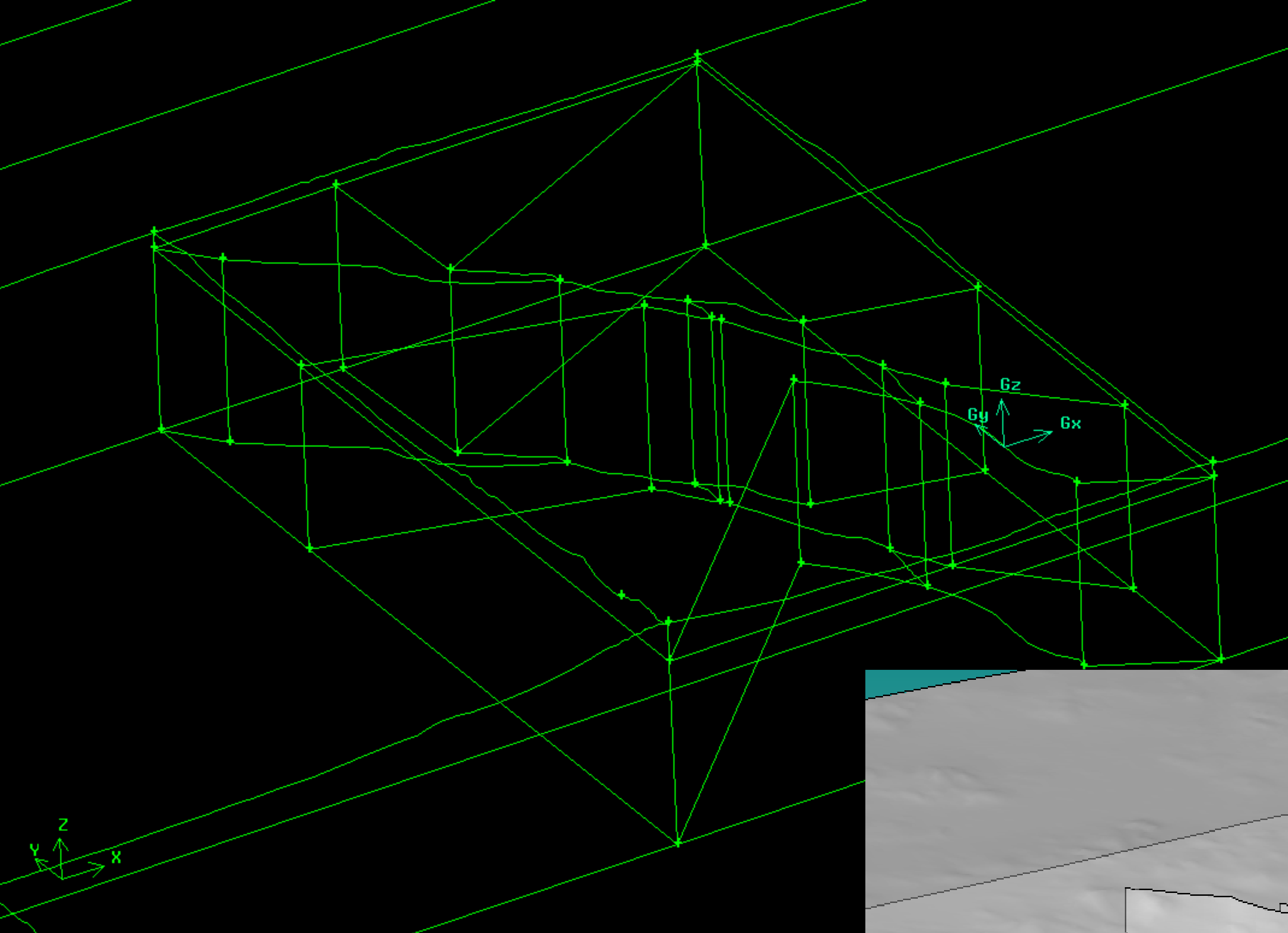

Gambit
vs
SimModeler

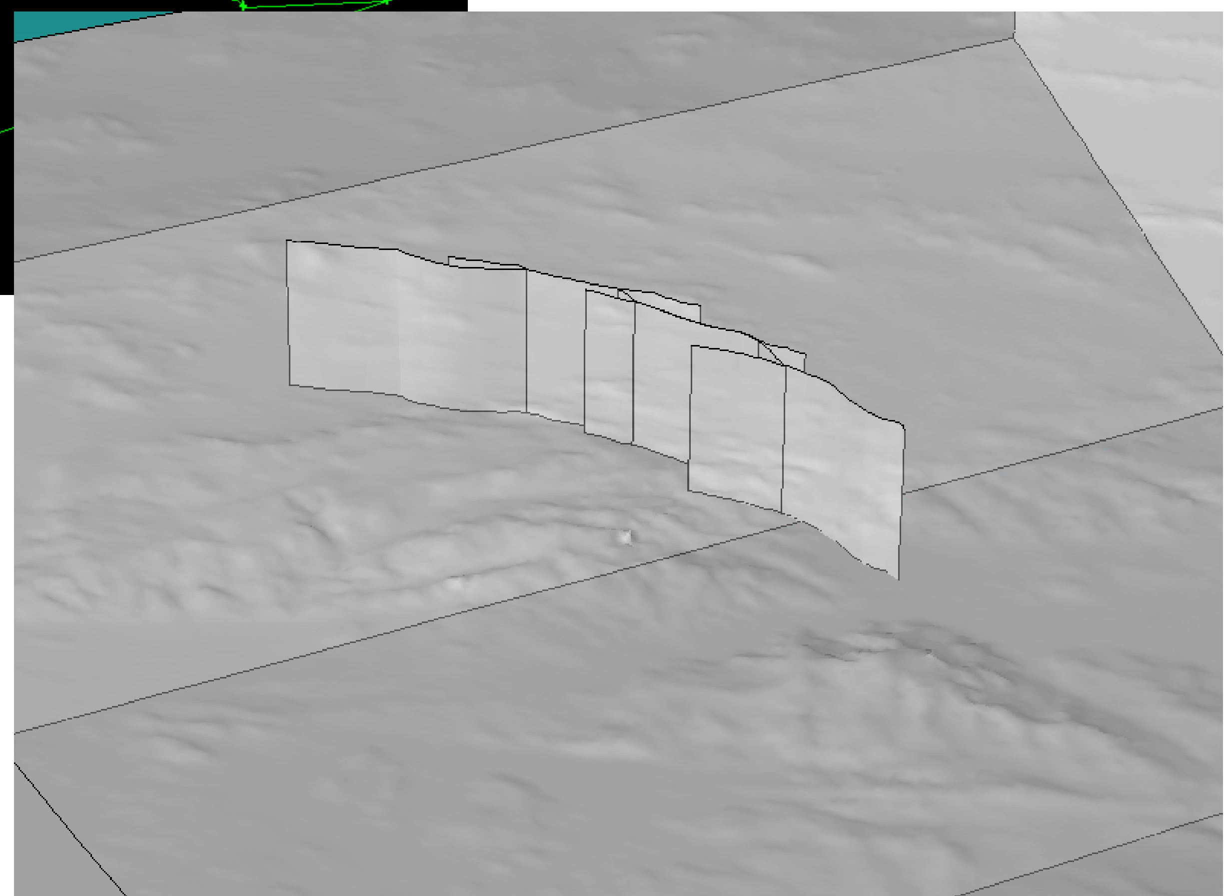

SimModeler

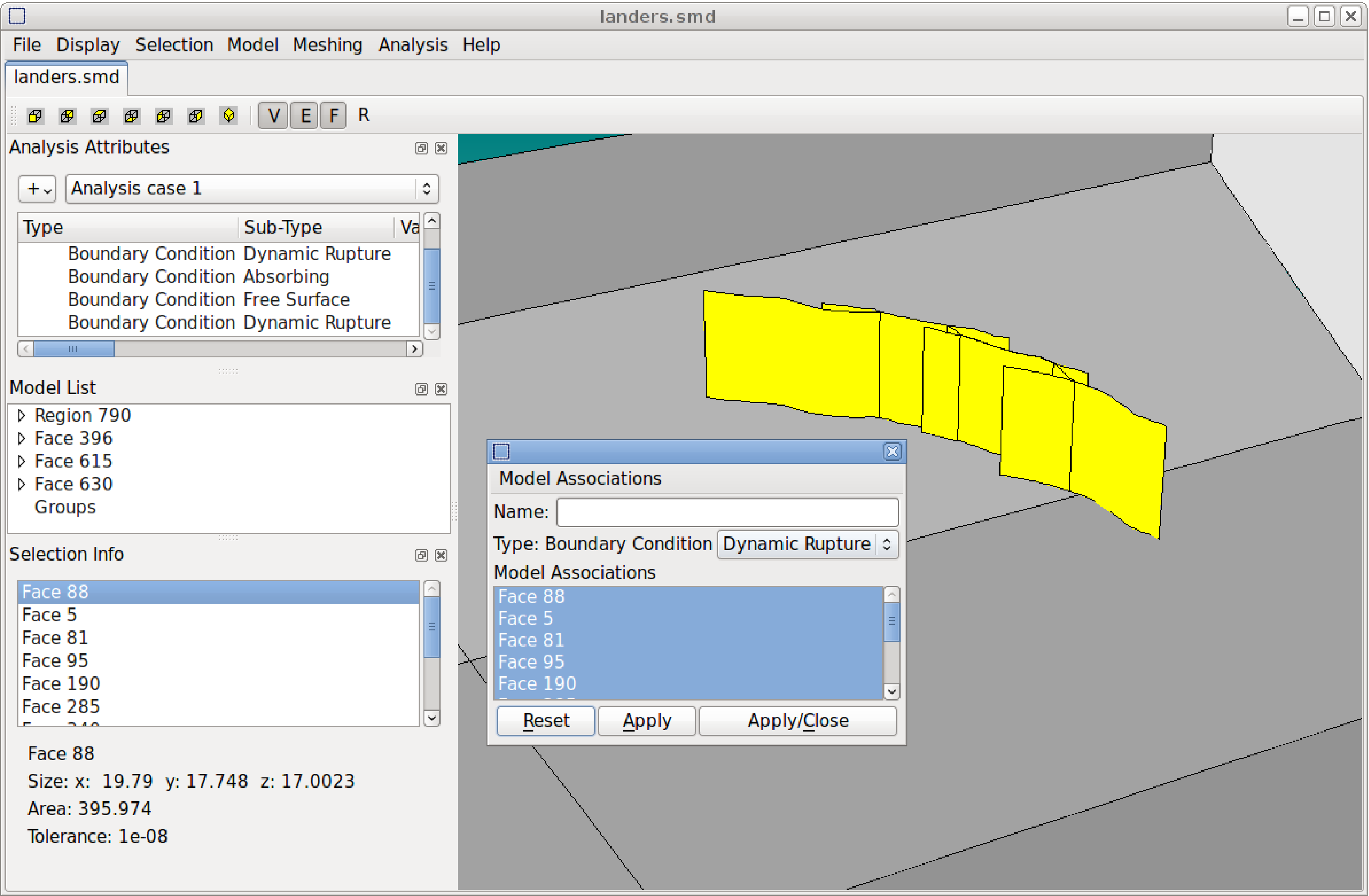

landers.smd
File Display Selection Model Meshing Analysis Help
landers.smd
V E F R
Analysis Attributes
Analysis case 1
Type
Sub-Type
Boundary Condition Dynamic Rupture
Boundary Condition Absorbing
Boundary Condition Free Surface
Boundary Condition Dynamic Rupture
Model List
Region 790
Face 396
Face 615
Face 630
Groups
Selection Info
Face 88
Face 5
Face 81
Face 95
Face 190
Face 285
Face 88
Size: x: 19.79 y: 17.748 z: 17.0023
Area: 395.974
Tolerance: 1e-08
Model Associations
Name:
Type: Boundary Condition
Dynamic Rupture
Model Associations
Face 88
Face 5
Face 81
Face 95
Face 190
Reset
Apply
Apply/Close

Example – The Mw 6.7 1994 Northridge earthquake

- Sixty killed, >7,000 injured, 40,000 buildings damaged, 44 Billion $ loss
- Blind thrust earthquake which was felt over 200,000 km^2 in US and Mexico
- High accelerations (1g), exceeding building codes
- Well recorded and studied

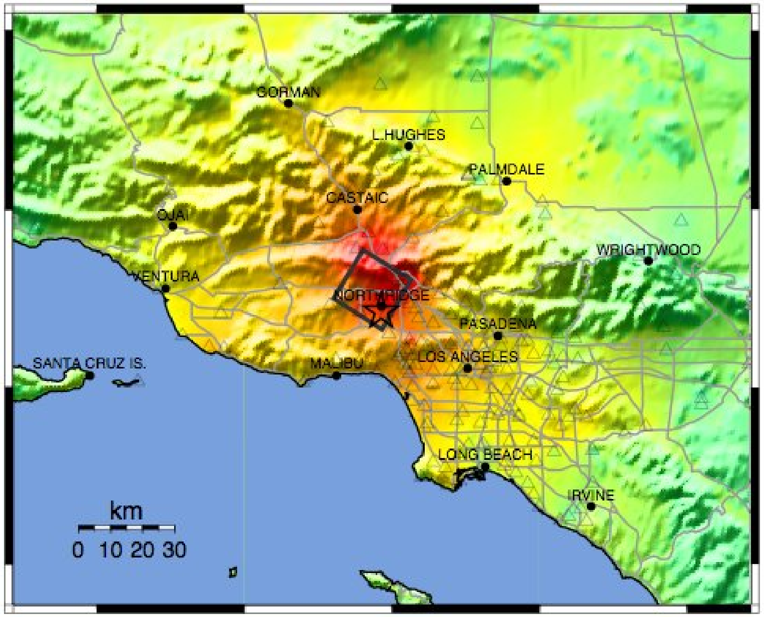

PERCEIVED SHAKING	Not felt	Weak	Light	Moderate	Strong	Very strong	Severe	Violent	Extreme
POTENTIAL DAMAGE	none	none	none	Very light	Light	Moderate	Moderate/Heavy	Heavy	Very Heavy
PEAK ACC.(%g)	<.17	.17-1.4	1.4-3.9	3.9-9.2	9.2-18	18-34	34-65	65-124	>124
PEAK VEL.(cm/s)	<0.1	0.1-1.1	1.1-3.4	3.4-8.1	8.1-16	16-31	31-60	60-116	>116
INSTRUMENTAL INTENSITY	I	II-III	IV	V	VI	VII	VIII	IX	X+

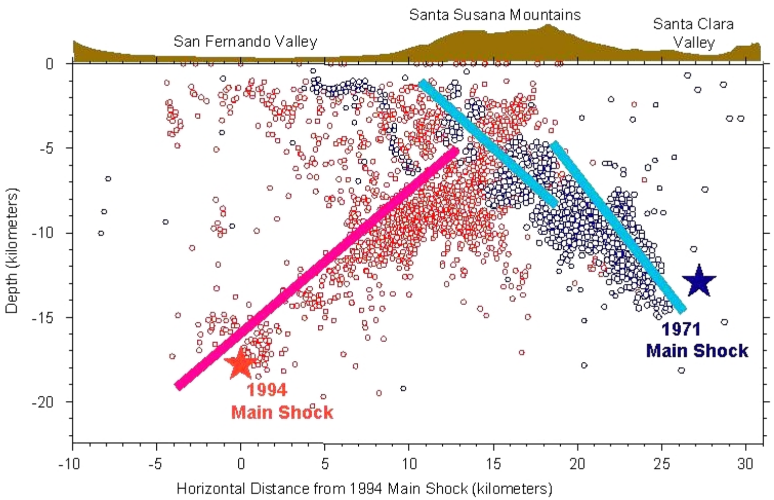

Example – The Mw 6.7 1994 Northridge earthquake

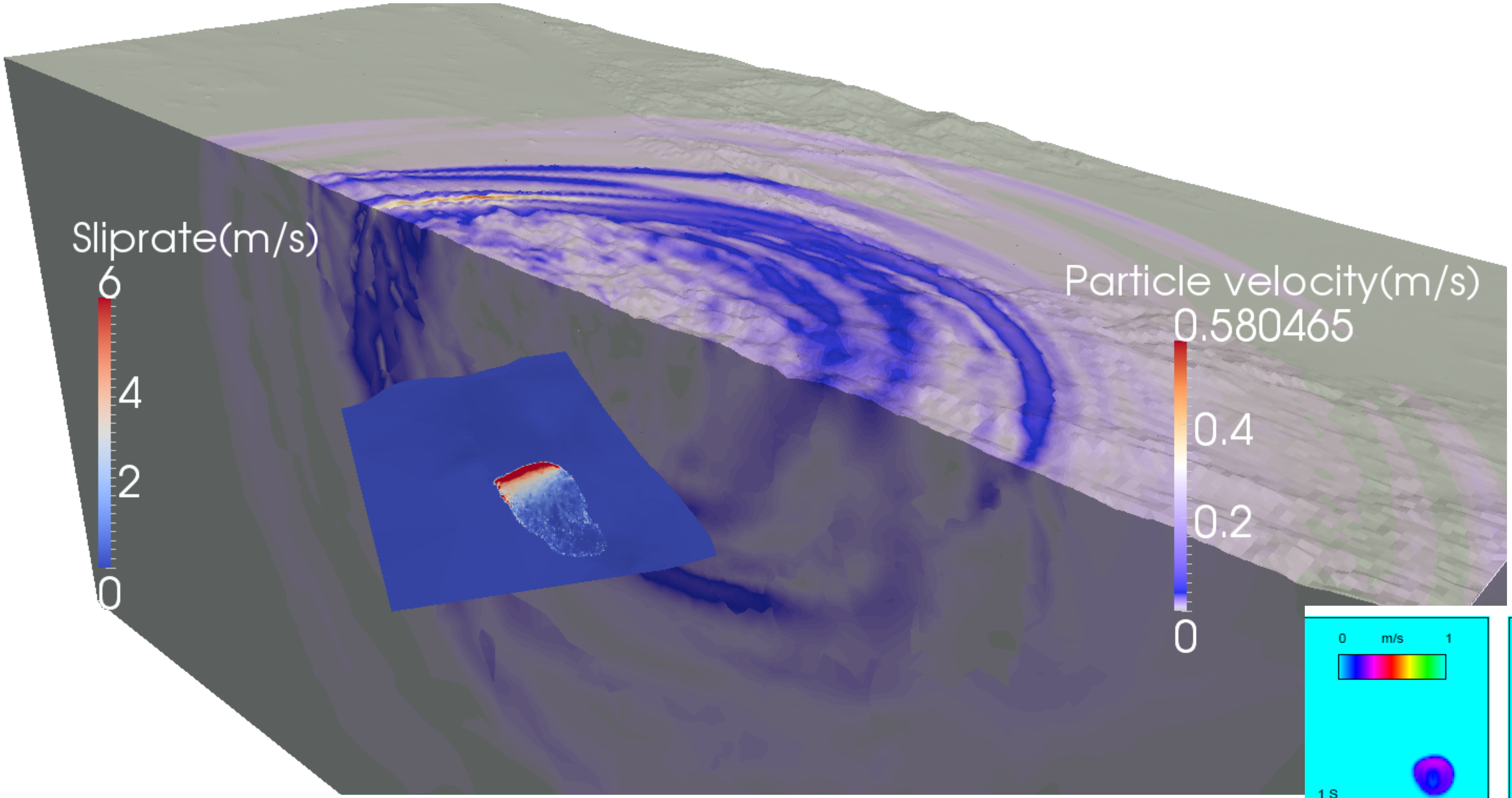

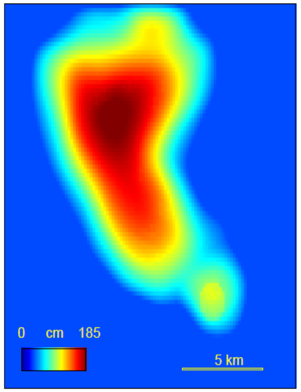

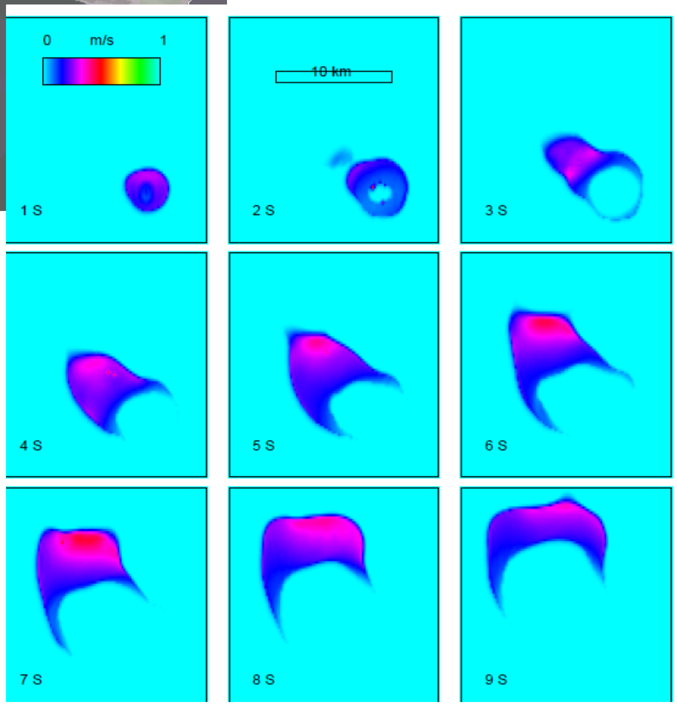

Compare final slip and slip rate from homogeneous dynamic rupture simulation on planar dipping fault with rate-and-state friction (Olsen et al., 1998)

Work by A. Gabriel

Conclusion & Outlook

- ADER-DG solver ready, functional and benchmarked
- Bring all features into production version (under construction)
- Combine dynamic rupture with local time stepping
- I/O improvements necessary (HDF5, under construction)
- Optimization on-going (serial performance, LTS load balancing)
- Toolbox in quite good shape
- Current bottleneck CAD generation (?)
- More Physics (plasticity), applications
- Open Source (soon), already available through http://verce.eu/

http://seissol.geophysik.uni-muenchen.de/

“Under which conditions do undersea earthquakes generate devastating tsunamis?”

(Jörn Behrens,
KlimaCampus, Universität Hamburg,
Numerical Methods in Geosciences)

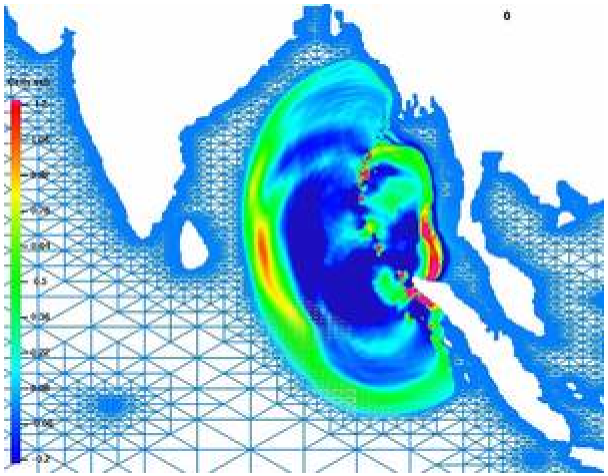

Failure criterion

Rate-and-state dependent friction

Implementation of rate-and-state friction

- Updating scheme includes Newton-Raphson search for slip rate and two iterations for state variable (Kaneko et al., 2008)

Velocity-stepping experiment of Niemeijer et al. (2010)

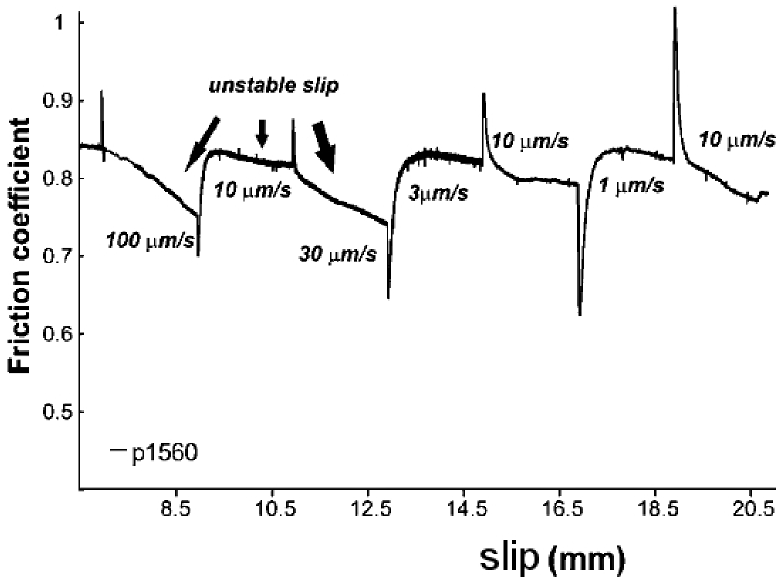

$$\mu_f = \mu_0 + a \ln \frac{v}{v_0} + b \ln \frac{v_0 \theta}{D_c}$$
$$\dot{\theta} = 1 - \frac{v\theta}{D_c}$$

θ state variable
a direct effect
b evolution effect
v_0 steady-state reference velocity
μ_0 steady-state reference friction

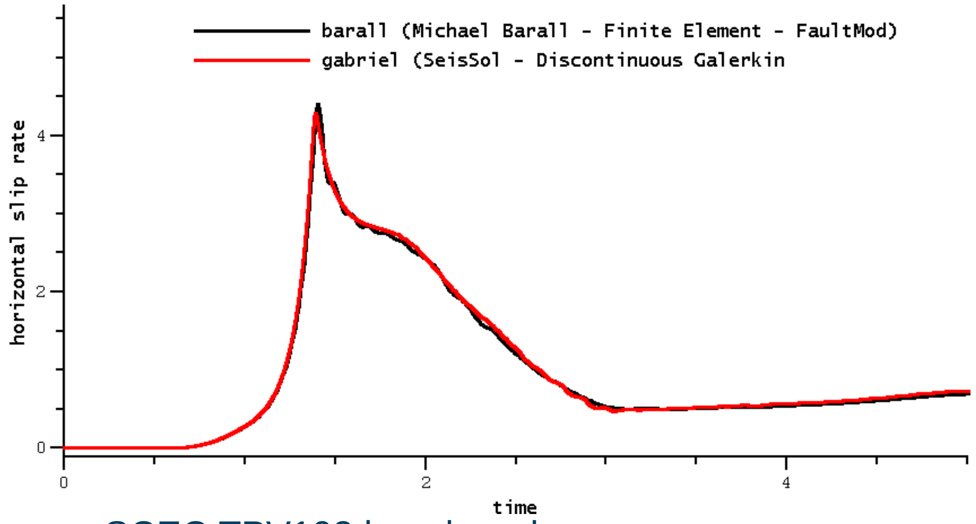

SCEC TPV102 benchmark

Dipping fault geometry

(SCEC Test Cases **TPV10** and TPV11)

- 60 degree dipping normal fault geometry
- Initial stress linearly depth dependent
- **Subshear** / supershear rupture conditions

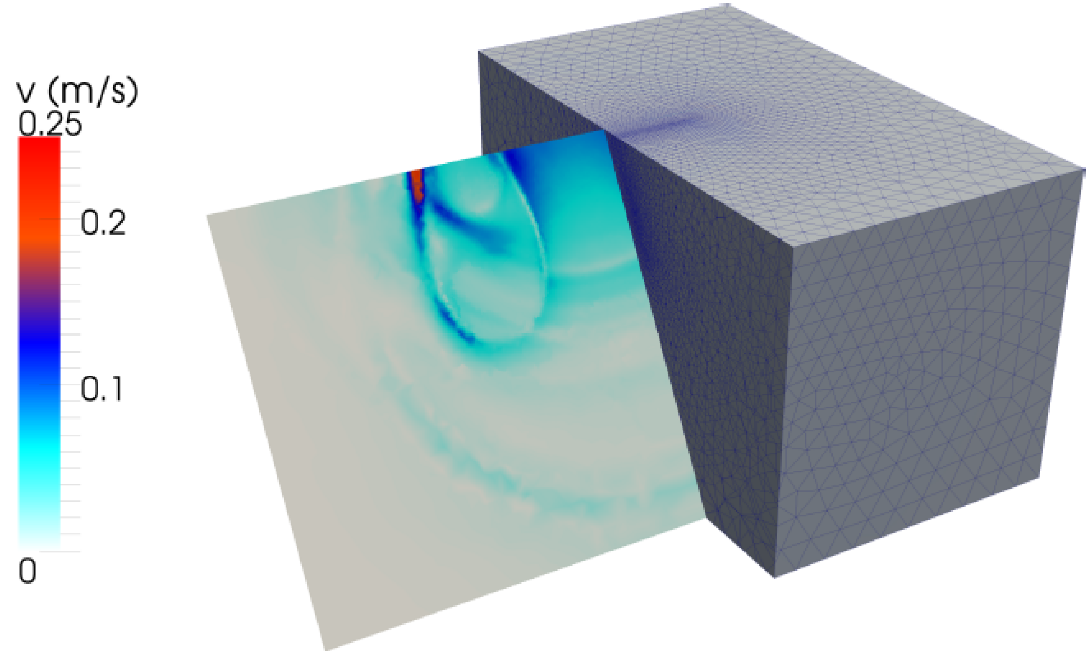

Mesh geometry, computational domain and particle velocity on the fault plane after ~9.6 s

Rupture time – contour plot (each 0.5 s)

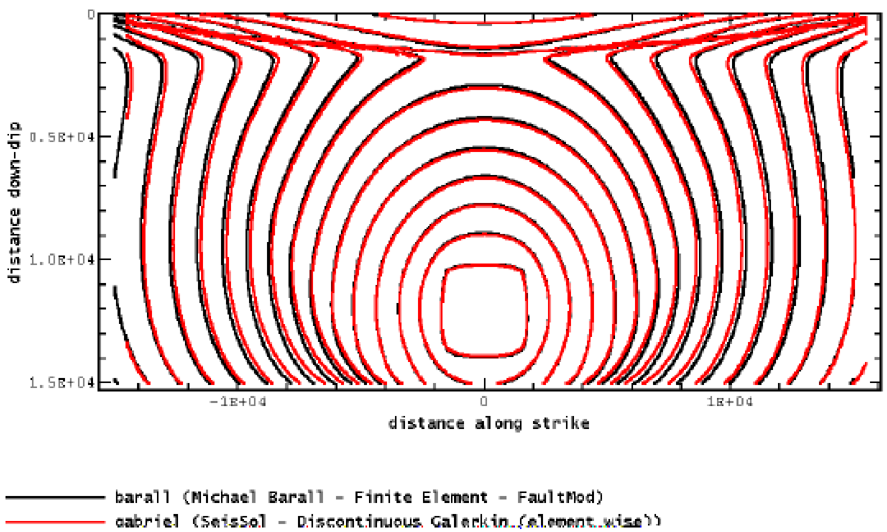

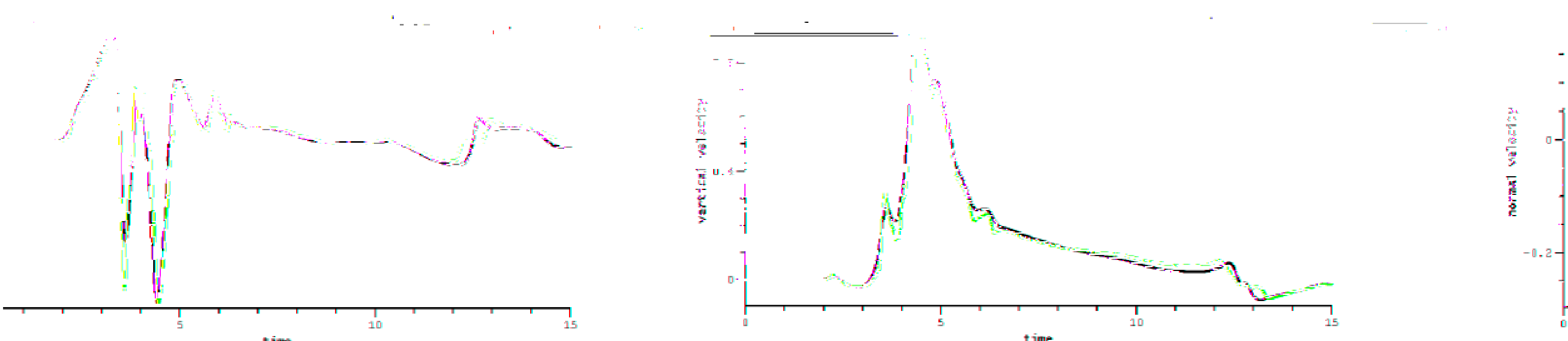

Heterogeneous background stress

(SCEC Test Cases TPV16 and **TPV17**)

onditions

irregular

- Randomly-generated heterogeneous initial stress co
- Trilinear interpolation to map background values on distributed integration points

s)

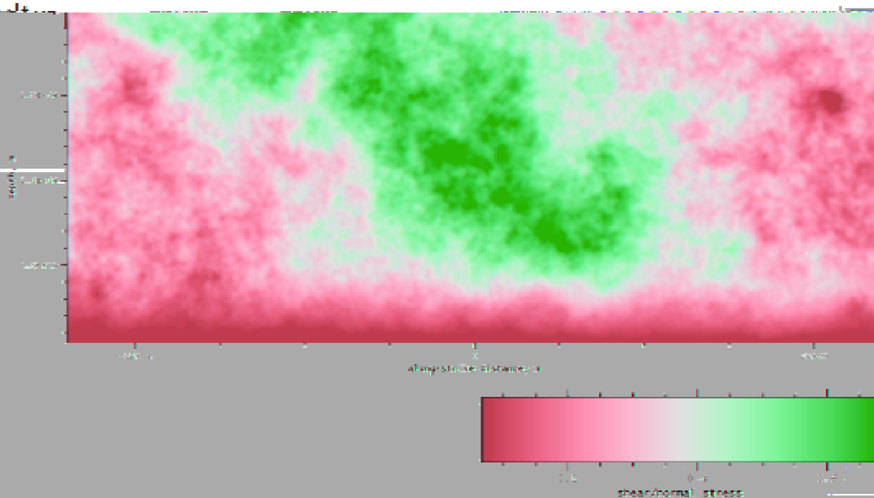

Initial shear stress on the fault plane

Rupture time – contour plot (each 0.5 s

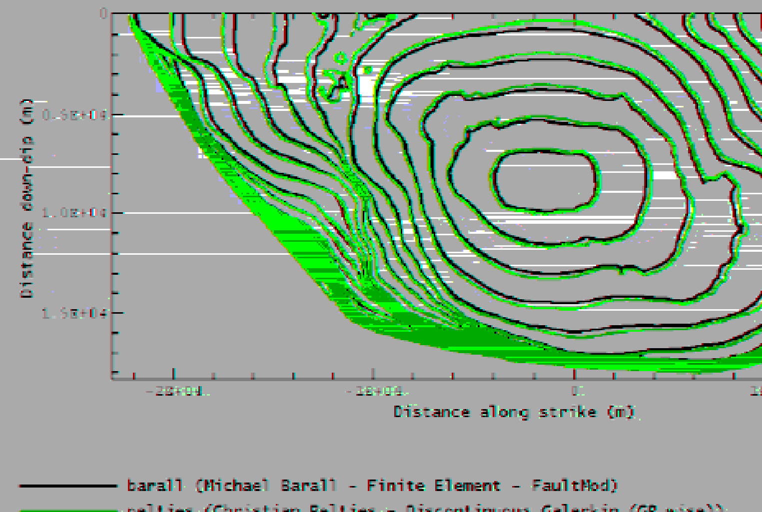

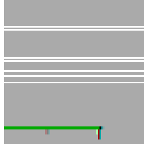

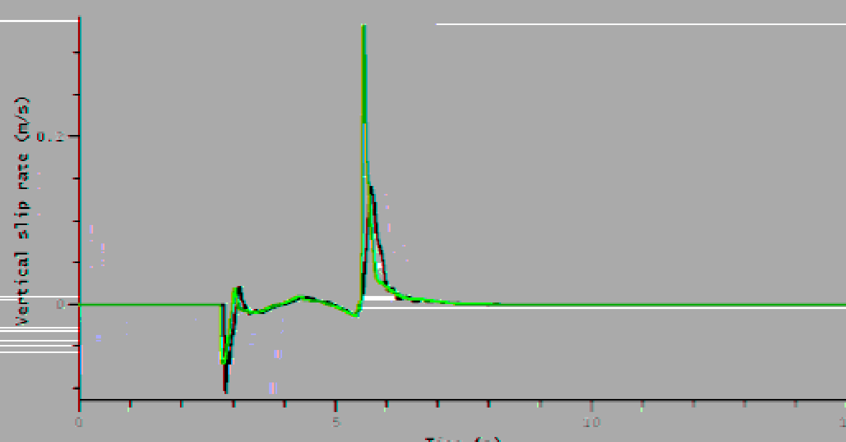

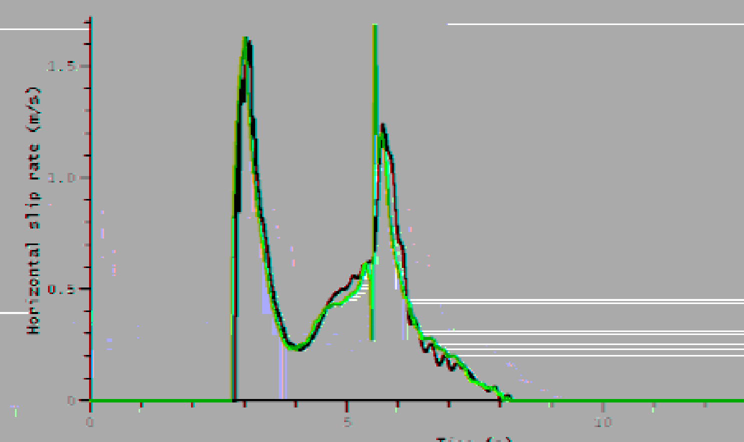

On- fault station
(strike -9.0 km, dip 9.0 km)

Fault branching geometry

(2D SCEC Test Cases TPV14 and **TPV15**)

- Left-lateral, vertical, strike-slip fault with a rightward branch forming a 30 degree angle
- Slightly stress-heterogeneous
- High resolution required

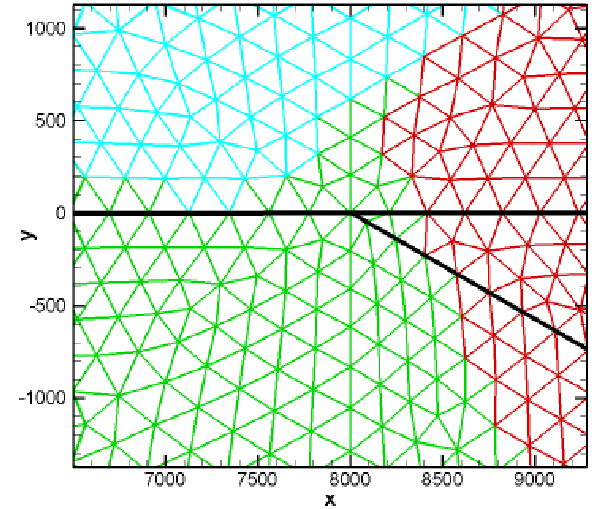

Junction point domain partitioning

Absolute particle velocity snapshots

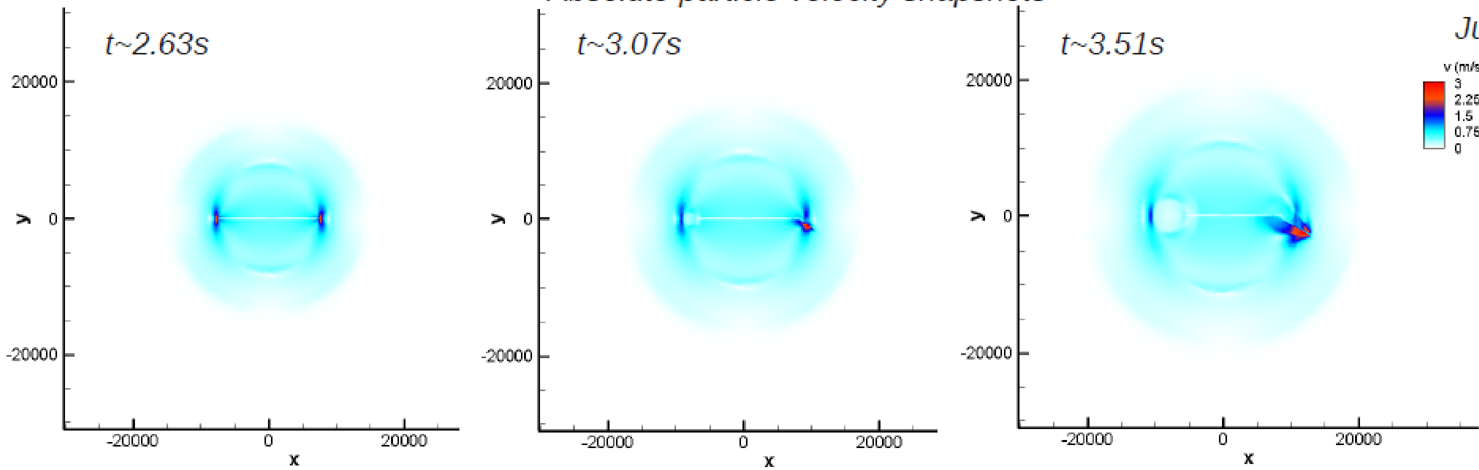

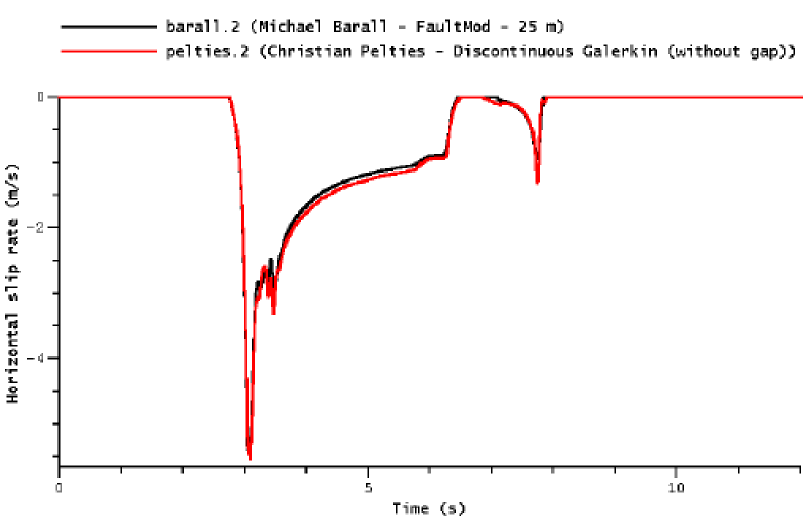

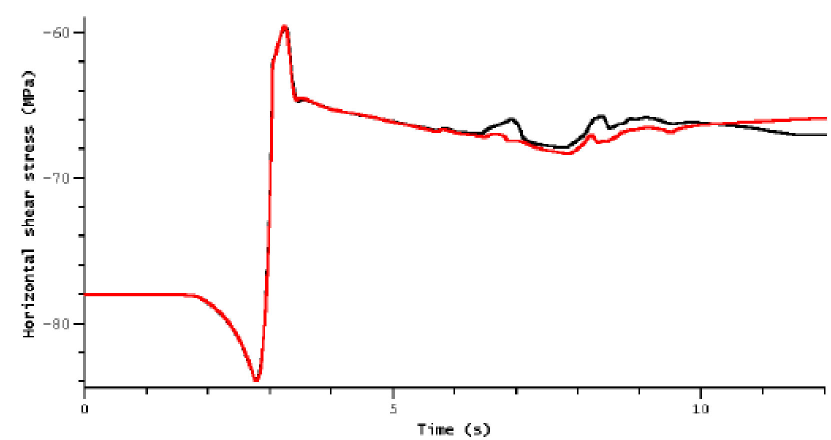

On- fault station
(branch, strike 2.0 km, dip 7.5 km)

By A. Nerger

Absence of Spurious Oscillations – Explanation Approach

Diffusion

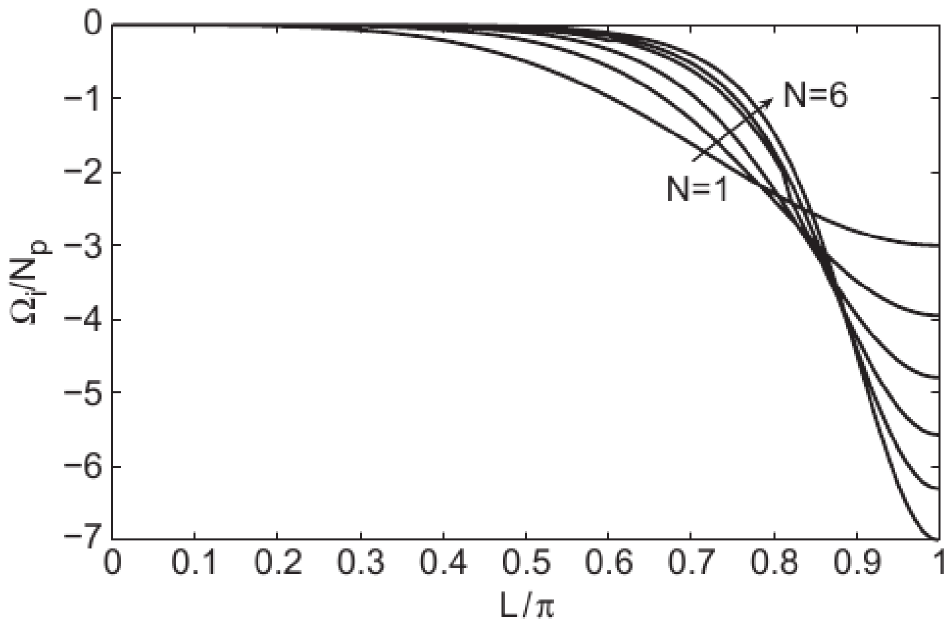

(Hesthaven and Warburton, 2008, p. 90, Fig. 4.1)

Higher frequency

- Numerical discretization includes numerical diffusion
- Numerical diffusion works in a desired and optimal way
- Damps unwanted high-frequency modes
- Does not affect longer, physically meaningful wavelengths
- But: Dispersion analysis for ADER-DG + DR to do!

Automated CAD generation – preliminary workflow

1. Download topography/bathymetry, e.g. from NOAA's ETOPO data collection
2. Define bounding box: rectangular or spherical
3. Material interfaces: structured grids of points
4. Faults: structured grids of points, gOcad's TS format
5. Check projection
6. (Triangulated) surface generation: Poisson surface reconstruction (MeshLab)
7. Assemble model: apply union, intersection, trimming operations with Simmetrix discrete modeling tools

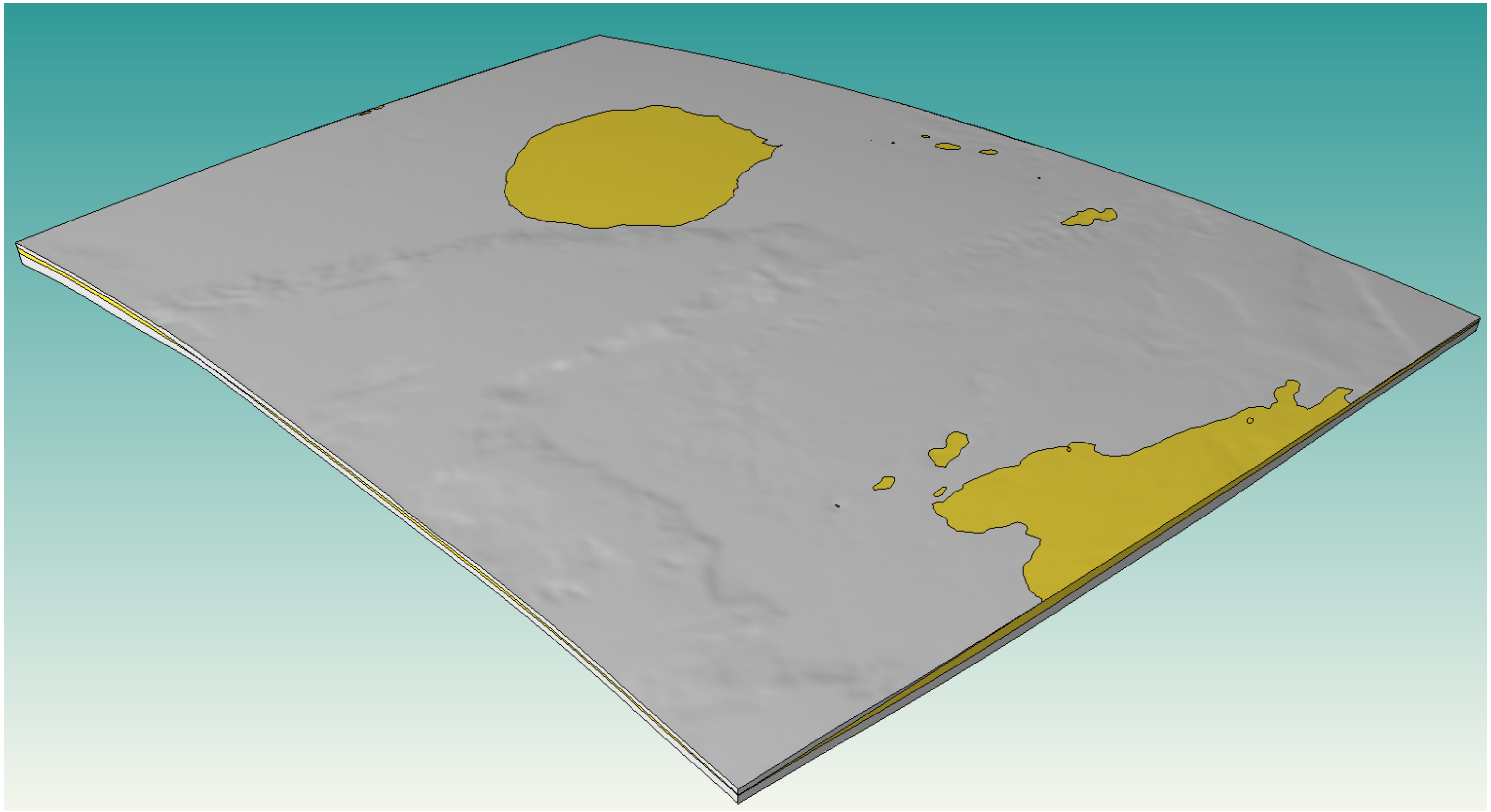

Biscay model, S. Wenk